

THE AGUACLARA STACKED RAPID SAND FILTER:
A NOVEL UNIT PROCESS AND FLUIDIC CONTROL
SYSTEM

A Thesis

Presented to the Faculty of the Graduate School
of Cornell University

in Partial Fulfillment of the Requirements for the Degree of
Master of Science

by

Michael James Adelman

August 2012

© 2012 Michael James Adelman
ALL RIGHTS RESERVED

ABSTRACT

Rapid sand filters are a familiar and mature technology, but their mechanical sophistication limits their sustainable application particularly in developing countries. Conventional rapid sand filters require pumps, elevated tanks, or multiple filter units to generate high flow rates for backwashing. Stacked rapid sand filtration is introduced here as a more robust and sustainable alternative. The AguaClara stacked rapid sand filter (SRSF) can backwash itself with no additional flow, which eliminates the need for pumps or other expensive equipment.

The first part of this study presents laboratory and field proof-of-concept demonstrations of this novel technology. The multi-layer configuration of the SRSF allowed a laboratory unit to be loaded at 1.4-1.83 mm/s (120-160 m/day) per layer and backwashed at 10-11 mm/s (860-950 m/day) with the same or similar total flow rate. The filtered effluent met U.S. EPA drinking water standards. The backwash cycle was also demonstrated, and flushing of contaminants from the sand bed was effective even with 5-10 NTU backwash water. A test stacked filter unit also demonstrated satisfactory filtration performance and effective backwashing at several water treatment plants in Honduras.

The second part of this study presents a novel control system for the SRSF based on fluidics. The fluidic control system, which permits changing from filtration to backwash modes of operation with a single valve, was developed in the laboratory and applied in the first full-scale SRSF. The water level in the filter is regulated by a siphon pipe, which conveys flow during backwash and which contains an air trap to block flow during filtration. The state of the siphon pipe and the ensuing state of the filter are controlled by a small-diameter air valve.

Biographical Sketch

Michael Adelman was born and raised in Clarks Summit, PA, where his interest in Legos and power tools started early in life and ultimately led him down the path to engineering. His nine years in Odyssey of the Mind exposed him to creative problem solving on a shoestring budget, and his exploration of abandoned mines and railroad tracks in the Scranton area led to his awareness of both local history and local environmental problems. This exploration also led to a world-class family collection of railroad spikes, tie plates, and date nails.

Michael went to Lafayette College in Easton, PA to study civil and environmental engineering. He had the good fortune to find an exciting field and a wonderful academic department, and his classes took him to all the best water plants, streams, landfills, and contamination sites in the Lehigh Valley. He worked with Dr. Art Kney and a team of dedicated students from the Lafayette Society of Engineers and Scientists to establish a campus-wide composting system that produces beautiful, humified compost to this day. Despite the long evenings collecting garbage from the dining halls and the long nights boiling it in the lab, the compost project was truly a labor of love. Michael was also a member of the Lafayette chapter of Engineers Without Borders, which took him to remote villages in the Yoro region of Honduras to work on gravity-fed water systems and agricultural empowerment ventures. He graduated with his B.S. in May 2010.

With the AguaClara program at Cornell University, Michael had the opportunity to once again be part of an incredible team. He has immensely enjoyed his work on the stacked rapid sand filter, and on other aspects of the AguaClara research from lamellar sedimentation to project governance. Four trips to Honduras with the AguaClara team have even given him the chance to visit those towns in Yoro again and taste coffee that he once helped plant.

This work is dedicated to my parents, Mary Beth and Harry Adelman, who showed me all the right paths in life and for whose love, patience, and support I am eternally thankful; and to Doña Reina Diaz Amador, the grandmother of all the AguaClara students who have spent time in Honduras.

Acknowledgments

The AguaClara stacked rapid sand filter (SRSF) was the ultimate team effort, and its development and success reflect the contributions of a great many people. I am grateful for the work that so many people put into this project and for the privilege of being a part of this team.

Thank you to my thesis committee members for their patience and support throughout this project. Dr. Monroe Weber-Shirk is truly remarkable for his vision of sustainable water treatment technology to address one of the world's most urgent needs, and for his tireless dedication to his vision and his students. His message of empowerment is really inspirational, especially because he lives it and does not just preach it. Dr. Len Lion has been a wonderful collaborator with the AguaClara research, and he brings his keen insight and years of research experience to the team - not to mention his incredible patience for editing documents and grant proposals. It has been a real honor to work with Dr. Marcela González Rivas as well. She brings a unique and valuable perspective to a team of mostly engineers, which has helped AguaClara forge what I believe will be a long and fruitful relationship with the School of City and Regional Planning.

An enormous and special thank you to Anderson Cordero, Jeff Will, and Will Maher, my three closest colleagues on the stacked filtration team. Anderson helped build the first ever SRSF in the lab and played a huge role in the proof-of-concept research. By May 2011, he had already graduated with his M.Eng. and lined up a new job - but he went above and beyond the call of duty and spent the summer of 2011 working in Honduras to bring the SRSF to scale. It was great to have a colleague who was not only so dedicated and capable, but also a fellow Red Sox fan - I could not have asked for more! Jeff was a key member of the lab team that demonstrated the SRSF; the design team that produced a remarkable set of

hydraulic calculations to take it to scale; and the implementation team that made it happen. It is hard to imagine someone doing more for the filter project in more different areas, and I just hope he was not too annoyed by my constant emails and questions over g-chat. Will was a member of the SRSF research team for several semesters, and his fabrication skills were really invaluable in putting together the first version of the fluidic control system. He helped us learn a great deal about many different aspects of the new filter, and his bocce ball set was also greatly appreciated.

The original off-the-wall idea of stacking layers in a rapid sand filter was developed by the AguaClara Filtration Team in Spring 2010, and it is their bold proposal that ultimately turned into this project. Thank you to Yoon Choi, Caroline Evans, Sarah Stodter, Rachel Philipson, and C. Collin Hollister for not being afraid to dream big.

A number of students have been a part of the lab research that went into this project. Though there have been many frustrations and many spills to be mopped up along the way, we have learned a great deal about practical and fundamental aspects of stacked filtration as a result of their effort. It has been my pleasure to work in the lab with Sarah Stodter, Jonny Ayala, Mike Liu, Sara Coffey, Dylan Guelig, Ziyao Xu, Alli Hill, Min Pang, Jordanna Kendrot, Eva Johnson, Bill Kuzara, Michelle Wang, Stephanie Lohberg, Chris Holmes, Danhong Luo, Weiling Xu, and Huifei Wu.

The AguaClara design team has also contributed a great deal to the development of this new technology. It is one thing to propose an idea and test it in the lab, and quite another to produce a scalable design - and the Mathcad sheets and AutoCAD drawings that produced the first full-scale SRSF in Támara were a truly remarkable accomplishment. Thank you to Mayssoon Sharif for her out-

standing work over the summer of 2011, producing version after version of the filter drawings as things kept changing in the field. Thanks also to Drew Hart and Andrew Sargent for their contributions to the calculations and design drawings.

Our colleagues at Agua Para el Pueblo in Honduras did an outstanding job in their effort to turn this project from idea into reality. Special thanks to Santiago Garcia for his site and structural designs, and for his enormous contributions to managing the implementation of the SRSF over and above his many other responsibilities. Thank you also to the rest of the staff - social technician Antonio Elvir, secretary Beatriz Molina, motorist Roger Miranda, AguaClara engineers Daniel Smith and Sarah Long, and directors Jacobo Nuñez and Arturo Diaz. Anderson and I really enjoyed living and working in Tegucigalpa with them for the summer.

Many members of the community of Támara, Francisco Morazán, Honduras played an important role in making this project happen. The municipal Water Board showed real trust and courage in partnering with us to build something that was the first of its kind in the world, and the full-scale SRSF would not have been possible without their dedication of significant time and resources. Thank you to Water Board president Juan Ramón “Moncho” Rivera, secretary Claudia Calderón, treasurer Julio Borjas Medina, and auditor Vicente Dominguez for all their effort. Thank you to Don Hector and his crew for their outstanding work on the construction of the filter - they overcame numerous challenges to build something that had never been built before, and in the end the real filter looked even better than the CAD drawings! Thank you to Daniel González at the Maresa hardware store - it seemed like we always needed either some new part or a jumpstart for the pickup truck, and he was always there either way. A special thank you to Támara water plant operator Antonio Cerrato for his assistance throughout the process of construction, testing, and troubleshooting. I was extremely impressed

with how quickly he learned to operate the filter, and how well he has done making it work and handling the problems that inevitably accompany a new technology into the field. Thank you to Doña Sonya for welcoming us and providing us a place to stay in Támara. Finally, a most heartfelt thank you to Doña Reina and her family for becoming our family in Honduras. It was a real joy for Anderson, Jeff, and me to spend time with you and get to know you.

It has been a real joy to be a part of the AguaClara team as well, and I want to thank my fellow grad students Karen Swetland and Matthew Hurst for their consistent support and willingness to help out, especially when I was tied up with grading or running on very little sleep. Thanks also to the student team leaders Rachel Philipson and Julia Morris for their enthusiastic and capable leadership. A number of other people in the School of Civil and Environmental Engineering were really helpful to the project as well. Whenever we needed to set up something in the lab or develop a fabrication method for the field, Paul Charles and Tim Brock in the machine shop always had a solution. Dr. Po-Hsun Lin also provided valuable advice from his extensive knowledge of rapid sand filtration.

Financial support for the lab research was provided in part by the U.S. EPA through several “People, Prosperity, and the Planet” grant awards. The field implementation of the SRSF was funded by the Sanjuan Foundation and the Támara Water Board, and my work in Honduras for the summer of 2011 was supported by the funding partners of the Environmental Engineers of the Future scholarship.

CONTENTS

1	Introduction	1
2	Stacked Filters: a Novel Approach to Rapid Sand Filtration	3
2.1	Abstract	3
2.2	Background	4
2.3	Process Theory	6
2.3.1	Traditional rapid sand filter design	6
2.3.2	Stacked rapid sand filter geometry	7
2.3.3	Stacked filter backwash hydraulics	10
2.3.4	Implications for design and applications	11
2.4	Materials and Methods	13
2.4.1	Laboratory stacked filter system	13
2.4.2	Control of parameters and data acquisition	14
2.4.3	Performance analysis	16
2.4.4	Field demonstration unit	17
2.5	Results and Discussion	18
2.5.1	Filtration cycle performance	18
2.5.2	Backwashing bed expansion	22
2.5.3	Contaminant removal during backwash	26
2.5.4	Use of settled water for backwash	27
2.5.5	Field demonstration results	28
2.6	Conclusions	30
2.7	References	31

3	A Novel Fluidic Control System for AguaClara Stacked Rapid Sand Filters	34
3.1	Abstract	34
3.2	Introduction	35
3.3	Materials and Methods	38
3.3.1	Pilot-scale apparatus	38
3.3.2	Control of parameters and data acquisition	40
3.4	Results and Discussion	41
3.4.1	Overall control system	41
3.4.2	Experimental evidence of mode transitions	42
3.4.3	Fluidic control of the mode of operation	45
3.4.4	Backwash siphon air trap hydrostatics	46
3.4.5	Backwash siphon air valve sizing	51
3.5	Conclusions	54
3.6	References	55
4	Overall Conclusions and Implications	57
4.1	Conclusions of the Two Studies	57
4.2	Future Work for Laboratory Research	57
4.3	Future Work for Field Implementation	60

LIST OF FIGURES

2.1	Conceptual diagram of flow in a six-layer SRSF system during (a) filtration mode and (b) backwash mode, showing both the division and the direction of flow in the filter bed. Note that both cycles can be run at the same total flow rate.	8
2.2	Schematic for the experimental SRSF system, showing a six-layer SRSF column along with the apparatus for alum and clay dosing; the pressure sensors to measure filtration and backwash head losses; and the influent and effluent turbidity sampling systems.	13
2.3	Diagram of the SRSF field demonstration unit showing its connection to the water treatment plant sedimentation tank. The flow directions and head requirement for the backwash cycle are shown here to illustrate the constraint on vertical placement of this filter. The filter bed is drawn in expanded form, but note that the height H_{Filter} is defined as the settled bed height.	19
2.4	Data from an example filtration cycle run at 144 m/day. The three regions demarcated on these graphs are (A) a ripening period, (B) a period of good filter performance, and (C) a decline in turbidity removal. Note that these regions are demarcated with respect to the U.S. EPA drinking water standard of 0.3 NTU.	21
2.5	Plot of expanded porosity for increasing backwash velocities, showing experimental data points and a power-law regression equation. The initial porosity of the bed when fully settled during a filtration cycle was 0.4, and expanded porosity was calculated from measured bed expansion using Eq. 2.8.	23

2.6	Configuration of the inlet valves of an SRSF to fluidize (a) two layers, (b) four layers, and (c) all six layers. When the inlet valves are set such that the entire backwash flow is passing upwards through a pair of layers, these layers will fluidize because they are experiencing the full backwash velocity.	25
2.7	Plot of effluent turbidity over time during a 950 m/day backwash cycle. The readings from the backwash turbidimeter were scaled by the sampling system dilution factor to produce the curve shown in this graph.	26
2.8	Results of the first SRSF field demonstration at the Támara water treatment plant in Francisco Morazán, Honduras, where the filter was loaded at 160 m/day with sedimentation tank effluent for around 1 hour to gauge the turbidity-removal performance of the system.	29
3.1	Diagram of flow in the sand bed of an SRSF during (a) filtration and (b) backwash. Note that the total incoming flow rate Q_{Plant} is the same during both cycles of operation.	37
3.2	Pilot-scale experimental apparatus including an SRSF column, inlet and outlet boxes, a backwash siphon, an air valve, and pressure sensors. Note that the water levels shown here are for the filtration cycle.	39
3.3	Fluidics control system for the SRSF, showing water levels during (a) filtration and (b) backwash. Important head losses during each cycle are also identified.	41

3.4	Water level traces from the pilot-scale apparatus, showing the water level change in the inlet box during the change from filtration to backwash and the return to filtration mode of operation.	43
3.5	Diagram of flow and water levels in the siphon pipe and key dimensions, including (a) during the backwash cycle, (b) just after the siphon is broken to end backwash, and (c) after water has risen to the clean-bed filtration height.	46
3.6	Diagram of (a) dimensions and (b) observed water levels for the laboratory-scale siphon system. The water in the filter column was allowed to rise a height H_{Rise} over the top of the sand, and the lengths a , b , and c were measured.	50

LIST OF TABLES

2.1	Process variables and typical values in single-media rapid sand filters.	7
2.2	Comparison of SRSF with conventional rapid sand filtration alternatives.	12
2.3	Bench-scale SRSF performance under various filtration-cycle conditions.	20
2.4	Observed bed expansion at two backwash velocities.	24
3.1	Predicted and measured values of a and b in the experimental siphon, given H_{Rise}	51

CHAPTER 1

INTRODUCTION

The stacked rapid sand filter (SRSF) is a novel unit process invented by the Cornell AguaClara program. It is a self-backwashing filter: a single SRSF unit can carry out the filtration and backwash cycles at the same flow rate without the requirement for pumps, elevated tanks, or multiple filter boxes. Its development was motivated by the global need for more robust and sustainable municipal-scale water treatment technology. Consistent with the design philosophy of AguaClara, the SRSF runs entirely by gravity. The AguaClara program as a whole seeks to design more affordable water plants carrying out chemical dosing, rapid mix, flocculation, sedimentation, filtration, and disinfection, and thus improve potable water service in cities and towns around the world.

The SRSF required two key innovations: a *new geometry* of the sand bed in a rapid sand filter, with inlets and outlets spaced throughout the bed to make six layers that would filter in parallel and be backwashed in series; and a *new control system* to provide the flow patterns required by this novel geometry. This thesis consists of the development and testing of these two innovations, and the research described here served to demonstrate the viability of the SRSF and ultimately bring it to full scale.

The first part of this thesis (Chapter 2) describes the sand bed geometry of the SRSF. The process theory is discussed to explain how the SRSF carries out filtration and backwash at the same flow rate while still maintaining filtration and backwash velocities in the typical design range for rapid sand filtration. A laboratory system was used to test the filtration and backwash cycles in the SRSF, to show that it was possible for an SRSF to achieve adequate performance during filtration and effective contaminant removal during backwash.

The second part (Chapter 3) describes an innovative system of fluidics to control the SRSF. The fluidic system uses one air valve to control flow to four inlets and three outlets and thus set the mode of operation of the SRSF. The central element of this system is a backwash siphon pipe, which conveys flow during backwash and contains an air trap to block flow during filtration. The fluidic control system was tested in the laboratory, and at the first full-scale installation of the SRSF in Támara, Francisco Morazán, Honduras.

Chapter 4 summarizes the major conclusions from this research and suggests areas that may benefit from additional investigation. The SRSF has realized encouraging success to date, but there remain a number of interesting topics for both laboratory and full-scale research.

CHAPTER 2

STACKED FILTERS: A NOVEL APPROACH TO RAPID SAND FILTRATION

2.1 Abstract¹

Rapid sand filters are a familiar and mature technology, but the mechanical sophistication they incorporate in industrialized nations limits their sustainable application in developing countries. Conventional rapid sand filters require pumps, elevated tanks, or multiple filter units to generate high flow rates for backwashing. Stacked rapid sand filtration is introduced here as a more robust and sustainable alternative. A stacked rapid sand filter can backwash itself with no additional flow, which eliminates the need for pumps or other expensive equipment. This study presents laboratory and field proof-of-concept demonstrations of this novel technology. The multi-layer configuration of stacked rapid sand filters allowed a laboratory unit to be loaded at 1.4-1.83 mm/s (120-160 m/day) per layer and backwashed at 10-11 mm/s (860-950 m/day) with the same or similar total flow rate. The filtered effluent met U.S. EPA drinking water standards. The backwash cycle was also demonstrated, and flushing of contaminants from the sand bed was effective even with 5-10 NTU backwash water. A test stacked filter unit also demonstrated satisfactory filtration performance and effective backwashing at several water treatment plants in Honduras.

¹The contents of this chapter are in press for publication in the *Journal of Environmental Engineering*, with co-authors M.L. Weber-Shirk, A.N. Cordero, S.L. Coffey, W.J. Maher, D. Guelig, J.C. Will, S.C. Stodter, M.W. Hurst, and L.W. Lion.

2.2 Background

Untreated or insufficiently-treated surface water is responsible for a large portion of the health problems caused by poor water quality around the world (Mihelcic et al., 2009). The unit process sequence of flocculation, sedimentation, filtration, and disinfection effectively removes turbidity and pathogens from surface water in many municipalities in the industrialized world. However, municipal-scale drinking water treatment – even the familiar and reliable processes in a rapid sand filtration plant – have shown limited economic viability and technical effectiveness in many less developed areas of the globe (Whittington and Hanemann, 2006; Mintz et al., 2001). Large-scale water treatment processes have generally been developed for application in a ‘First World’ milieu where electric grids are reliable, technical expertise is available to support operation and maintenance, supply chains exist for replacement of machined parts, and communities have sufficient economic resources to afford sophisticated treatment systems. Water treatment projects outside of this context often face more difficult technical, material, or economic constraints (Hokanson et al., 2007; Ahrens and Mihelcic, 2006).

The development of more efficient water treatment processes also can benefit the industrialized world. Substantial investments will be needed to maintain and improve American water treatment infrastructure in the coming decades (ASCE, 2009), and the same is true in other developed countries. While many alternatives exist for water treatment (such as membrane processes), it is likely that rapid sand filtration plants will remain an important part of the technology portfolio for municipal-scale infrastructure. More sustainable and efficient processes for plants of this type will be desirable, especially with an increasing emphasis being placed on the energy costs and carbon footprint associated with water infrastructure (Stillwell et al., 2010).

Rapid sand filters are important in surface water treatment because they remove residual suspended solids following flocculation and sedimentation to produce low-turbidity effluent (Reynolds and Richards, 1996). Rapid sand filters also effectively remove pathogenic cysts such as *Cryptosporidium* (Gitis, 2008). Rapid sand filters are run in the forward (typically downflow) direction to remove solids from the influent water, and must be fluidized and backwashed for cleaning once the bed is fully loaded. One reason rapid sand filtration (as practiced in industrialized countries) is difficult to implement in resource-poor communities is that high flow rates are necessary to backwash filters, and achieving these flows requires one or more of the following:

- *Electric pumps.* High flow velocities can be achieved by pumping backwash water through the filter. Electricity for the pump, however, adds considerable operating cost, and pumping is impractical for communities without reliable electrical service.
- *Elevated storage.* A tank at a high elevation can be used to generate large flows for backwashing; however, the provision of an additional tank adds to the cost of the filtration system, and the volume of water typically consumed for backwash can significantly reduce the net volume of clean water produced.
- *Multiple filter units.* A bank of parallel filters is an alternative to pumps or elevated tanks. One filter can be taken offline for backwashing, and flow is diverted to this filter from all of the other filters to produce a high upflow velocity. Because the backwash velocity tends to be 6-7 times the filtration velocity, 7-8 individual filter units are needed, which adds to the capital cost and operational complexity of this scheme.

This study introduces a novel self-backwashing rapid sand filter for municipal scale water treatment. The stacked rapid sand filter (SRSF) presented here can operate

using the same volumetric flow rate for both filtration and backwash. Thus, the SRSF can be backwashed by gravity in any situation where a low elevation drain is available. The SRSF also has a smaller footprint and construction cost relative to multiple filter units. As a result, the SRSF is expected to be a robust and sustainable technology for municipal-scale drinking water facilities around the world. The objective of this study was to validate the SRSF concept in both laboratory and field experiments, by demonstrating adequate filtration-cycle performance and effective backwashing.

2.3 Process Theory

2.3.1 Traditional rapid sand filter design

There are two modes of operation for a rapid sand filter:

1. *Filtration.* Turbid water passes through the filter media and suspended solids are removed by transport and attachment to the sand grain surfaces (Yao et al., 1971). The filter operates in filtration mode until turbidity removal declines or until the head loss through the filter increases to an excessive level.
2. *Backwash.* Water passes through the filter in the reverse direction at a velocity sufficient to fluidize the filter bed media, detaching captured solids from the media and transporting them out of the filter. The filter operates in backwashing mode until the filter bed media has an acceptably low level of attached solids. At the end of backwashing, the filter media settles, and the filtration process begins again. Often, the filter is rinsed to remove any trace of backwash water before effluent is sent to clean water storage.

Table 2.1: Process variables and typical values in single-media rapid sand filters.

Variable	Unit	Typical Range	Reference
Loading rate	m/day	100 - 230	AWWA, 1971
Backwash velocity	m/day	860 - 1200	Davis and Cornwell, 2008
Influent turbidity	NTU	1 - 10	Davis and Cornwell, 2008
Turbidity removal	%	90 - 98	Reynolds and Richards, 1996
Bed depth	m	0.5 - 0.75	Reynolds and Richards, 1996
Media effective size	mm	0.35 - 0.70	Reynolds and Richards, 1996

In both filtration and backwash modes, the approach velocity or loading rate V is defined as the flow Q per unit area of the bed A_{Bed} , as in Eq. (2.1):

$$V = \frac{Q}{A_{Bed}} \quad (2.1)$$

Typical design parameters for single-media rapid sand filters are shown in Table 2.1.

2.3.2 Stacked rapid sand filter geometry

A stacked rapid sand filter consists of a sand bed in a single vessel, with inlets and outlets placed through the wall at several points to create multiple layers (see Fig. 2.1). During filtration mode, each layer of the SRSF receives a portion of the total flow and acts as an independent filter operating in parallel with the other layers. Depending upon its position relative to the influent and effluent piping, either downward or upward flow will occur through a layer. During backwash, the entire flow moves through the sand bed in the same direction from bottom to top and the layers are fluidized. Fig. 2.1 illustrates flow through a stacked filter column during both modes of operation.

In a traditional rapid sand filter, the approach velocity can only be changed by varying the total flow through the system. The stacked configuration of the SRSF allows for the scaling of loading rate and backwash velocity by the number

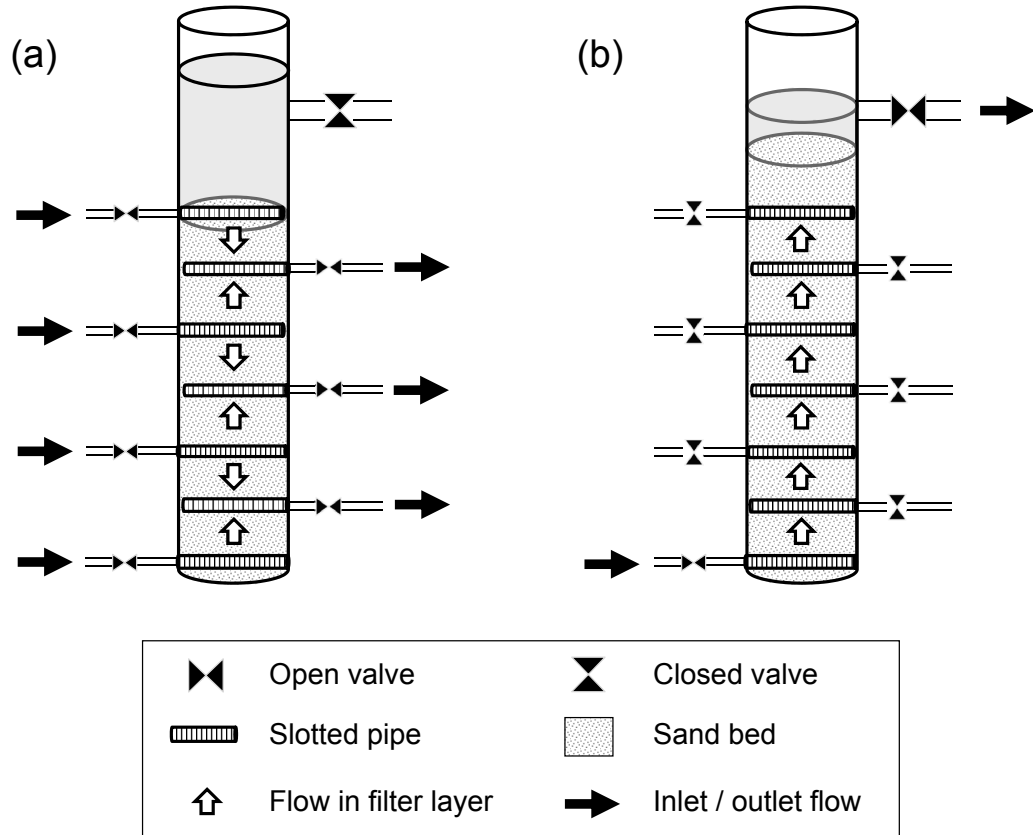


Figure 2.1: Conceptual diagram of flow in a six-layer SRSF system during (a) filtration mode and (b) backwash mode, showing both the division and the direction of flow in the filter bed. Note that both cycles can be run at the same total flow rate.

of layers, N_{Layer} . The layers of the SRSF operate in parallel during filtration mode, so the total flow is divided among the layers and the flow rate $Q_{Filtration}$ in each layer is:

$$Q_{Filtration} = \frac{Q_{Total}}{N_{Layers}} \quad (2.2)$$

This calculation assumes that each layer receives an equal share of the total flow. It is important to note that flow will be divided equally in parallel among several sand layers of uniform depth and composition, as long as head losses in the sand and not head losses in the inlet plumbing control flow distribution. The filtration cycle approach velocity $V_{Filtration}$ in each layer can be calculated by substituting Eq. (2.2) into Eq. (2.1):

$$V_{Filtration} = \frac{Q_{Total}}{N_{Layer}A_{Bed}} \quad (2.3)$$

In backwash mode, the total flow passes through all filter bed layers in series, so the number of effective layers is now $N_{Layer} = 1$. As a result, Eq. (2.3) becomes:

$$V_{Backwash} = \frac{Q_{Total}}{A_{Bed}} \quad (2.4)$$

Setting the flow rates equal in Eqs. (2.3) and (2.4) gives:

$$V_{Backwash} = N_{Layer}V_{Filtration} \quad (2.5)$$

Eq. (2.5) shows that the SRSF, unlike a traditional rapid sand filter, can use the same total flow rate for both filtration and backwashing, and the backwash velocity will still be N_{Layer} times greater than the filtration velocity. The number of layers in the SRSF can be selected based on the desired ratio of backwash velocity to filtration loading rate. Backwash velocities are typically around six times the filtration loading rate, so a six-layer SRSF satisfies this condition.

2.3.3 Stacked filter backwash hydraulics

The head $HL_{Backwash}$ required to backwash the SRSF can be approximated with the same relationship that is typically used to predict backwash head loss for a single-media rapid sand filter:

$$HL_{Backwash} = H_{Filter} (1 - \varepsilon) \left(\frac{\rho_{Sand}}{\rho_{Water}} - 1 \right) \quad (2.6)$$

where H_{Filter} is the settled depth of the sand, ε is the settled bed porosity, ρ_{Sand} is the density of the sand particles, and ρ_{Water} is the density of water (Davis and Cornwell, 2008). With typical parameters of $\varepsilon = 0.4$ and $\rho_{Water} = 2650 \text{ kg/m}^3$, the backwash head loss is 0.99 times (or roughly equal to) the height of the settled filter bed. This head requirement reflects the energy input needed to suspend the sand particles in the water column, and it is independent of velocity, provided that the upflow velocity is sufficient to fluidize the particles. Note that the backwash head loss in the SRSF may differ slightly from the prediction of Eq. (2.6). It may be higher because of minor losses around the inlet and outlet pipes that are placed through the sand bed, or it may be lower because some of the sand in the bed is displaced by these inlet and outlet pipes.

Successful operation of the backwash cycle for the SRSF requires the following conditions:

1. All flow enters through the lowest inlet pipe and exits at a point above the sand bed.
2. Water passes through the sand at a sufficient velocity. As long as the filter has been sized with Eq. (2.4) to provide a typical rapid sand filter backwash velocity, this velocity is expected to be sufficient to fluidize the sand and provide an adequate degree of expansion.
3. Sufficient head is available over the backwash exit point to suspend the sand

grains. This head should be approximately equal to the sand bed height with typical filter sand, plus any extra head required to overcome minor losses due to pipes in the sand bed.

2.3.4 Implications for design and applications

The costs associated with backwashing are an important limitation to the widespread application of rapid sand filters in municipalities in the developing world. As discussed above, the infrastructure required to backwash conventional filters represents a significant capital cost. In addition, backwash may require as much as 5-7% of the total volume of water treated by a conventional system (Nasser et al., 2002; Cornwell and MacPhee, 2001) which adds to the operating cost. Some studies have sought to reduce the net loss of water to backwashing by mixing some of the backwash water with raw water and recycling it through the treatment process (Yang et al., 2006). A survey of 362 water treatment plants in the U.S. revealed that 226 of these plants recycle their backwash wastewater (Arora et al., 2001).

The SRSF concept is a distinct and novel solution to the problem of improving backwash efficiency. Implementation of the SRSF into a drinking water treatment system presents a number of possible benefits over the implementation of a traditional rapid sand filter. Capital costs are expected to be lower, because the SRSF is self-backwashing and no pumps, elevated tanks, or redundant filter units are required. Operating costs and operational simplicity are also likely to improve, because the SRSF requires no electrical equipment, and the total flow rate to the filter need not be adjusted to start the backwash cycle.

The benefits listed above would make the SRSF a preferable option to traditional rapid sand filters for drinking water treatment in many parts of the world. If this novel technology is shown to be viable, it would realize gains in efficiency

Table 2.2: Comparison of SRSF with conventional rapid sand filtration alternatives.

Parameter	Unit	SRSF Design	Conventional Designs		
			Pumps	Storage	Multi-unit
Configuration		Sand bed with 6 filter layers	Pumps deliver backwash flow	Tanks provide backwash flow	7 filter units in parallel
Special equipment		Inlet / outlet manifolds	Electric pumps and controls	Elevated tank and valves	Header for flow control
Filter boxes	Number	1	1	1	7
Filter box area	m^2 per filter box	0.91	5.46	5.46	0.91
Filter cycle flow	L/s per filter box	10	10	10	1.4
Backwash flow	L/s	10	60.1	60.1	10

Note: Assumed plant capacity is 10 L/s. Assumed loading rates are 1.83 mm/s (160 m/day) for filtration and 11 mm/s (950 m/day) for backwash. Values marked in bold highlight the implementation advantages of the SRSF compared to conventional filters.

illustrated by the design example in Table 2.2. This table compares the overall dimensions and flows of the SRSF to conventional alternatives for a hypothetical 10 L/s water plant serving a few thousand consumers in a small city in the developing world.

Some water savings may also be realized by the SRSF system. The placement of inlets and outlets throughout the sand bed in an SRSF creates multiple points of high solids concentration at the end of a filtration cycle. All six filter layers are then backwashed in series with the same water, which should produce a very concentrated waste stream. The concentration of removed solids in the backwash water is anticipated to allow the backwash cycle to be completed in a relatively short amount of time at the same flow rate used for the filtration cycle, which would reduce the loss of treatable water to backwashing waste.

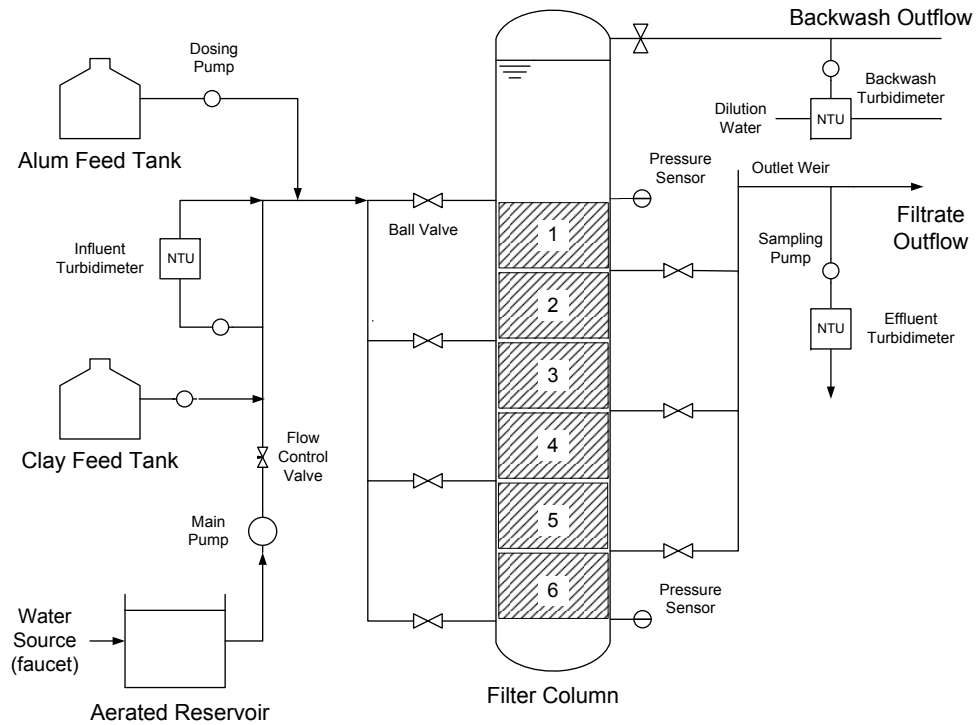


Figure 2.2: Schematic for the experimental SRSF system, showing a six-layer SRSF column along with the apparatus for alum and clay dosing; the pressure sensors to measure filtration and backwash head losses; and the influent and effluent turbidity sampling systems.

2.4 Materials and Methods

2.4.1 Laboratory stacked filter system

Two SRSFs (four-layer and six-layer) were constructed in 4" (10.16 cm) PVC pipe columns, with inlet and outlet pipes spaced to make 20 cm layers. The filtration and backwash cycles were demonstrated with simulated sedimentation tank effluent, using the system illustrated in Fig. 2.2. During filtration, the SRSF was loaded at 1.4-1.83 mm/s (120-160 m/day) per layer, in the range of typical design loading rates for rapid sand filtration. During backwash, similar flow rates were used to achieve upflow velocities of 10-11 mm/s (860-950 m/day) in all layers. These backwash velocities are also in the range of typical design values.

The layer inlets and outlets used $\frac{1}{2}$ " (1.27 cm) pipe with 0.008" (0.203 mm) well-screen slots (Big Foot Manufacturing, Cadillac, MI). Single slotted pipes were sufficient as the inlets and outlets in this small-diameter laboratory filter, because this laboratory filter column effectively had one inlet pipe for every 10 cm of filter width. Note that a full-scale SRSF would require slotted pipe manifolds to distribute flow through the sand. To promote uniform flow through the width of the filter layers, these manifolds should have a slotted pipe spacing smaller than the layer depth but large enough for flow to pass between the pipes during backwash. The ratio of pipe spacing (10 cm) to layer depth (20 cm) was 0.5 in this study; future research is needed to optimize this value for a full-scale design.

The head loss in the influent piping was limited to 10% of the head loss through the clean sand bed to promote uniform distribution of flow among the layers of the filter. Specifically, the piping components were sized such that their head losses were small compared to the frictional losses in the sand bed. The filter media was typical rapid sand filtration sand with an effective particle diameter of 0.45 mm and a uniformity coefficient of approximately 1.4 (Ricci Bros. Sand Co., Port Norris, NJ).

2.4.2 Control of parameters and data acquisition

The laboratory system utilized tap water from the Ithaca, NY municipal system (hardness \approx 150 mg/L as $CaCO_3$, alkalinity \approx 113 mg/L as $CaCO_3$, pH \approx 7.7; Foote et al., 2010). In a reservoir upstream of the SRSF, hot and cold water were blended to achieve a room-temperature mixture, and air was bubbled through the reservoir to strip any excess dissolved gas from the water.

The tap water was modified by addition of kaolin clay and alum to create a model sedimentation tank effluent, which a SRSF system would be treating in prac-

tice. Simulated settled-water turbidity in the range of 5-10 NTU (Nephelometric turbidity units) was maintained by mixing a concentrated clay stock solution into the influent. Water exiting a sedimentation tank at a coagulation-flocculation plant also typically contains residual coagulant, which is important for the effectiveness of the filtration process because it promotes attachment of suspended particles to the filter media (Yao et al., 1971). Therefore, 1.5 mg/L alum ($Al_2(SO_4)_3 \cdot 14H_2O$) was added to the filter feed water by dosing from a concentrated stock. This simulated settled water was used for filtration cycles, and also for several backwash cycles as a field-scale SRSF might be used.

In-line data logging turbidimeters (MicroTOL, HF Scientific) were used to monitor the influent and effluent turbidity and to assess filter performance. Samples were continuously pumped through the turbidimeters at greater than 0.83 mL/s to prevent settling of particles in the sample lines. A dilution stream of clean water was pumped into the backwash turbidimeter at a constant flow rate to achieve a dilution factor of 9.9, so that the high turbidity in the backwash water could be measured within the turbidimeter's detection range.

Head loss across the filter bed was continuously measured and logged using an electronic pressure sensor with computer data acquisition, installed in the column just above the top of the sand bed as shown in Fig. 2.2. This sensor measured the height of water from its own elevation to the free water surface in the filter column. The sensor was zeroed when the water was at the level over the outlet weir reflecting the clean bed head loss, so that it tracked the increase in head loss over the course of a filtration cycle as suspended solids accumulated in the bed of the filter. Note that because there are multiple parallel paths through layers of the stacked filter, the filtration cycle head loss is equivalent to the head loss through any one path.

A second pressure sensor was placed at the level of the bottom inlet to the SRSF as shown in the Fig. 2.2. This sensor was used in conjunction with the first pressure sensor to measure the head loss across the sand bed during the backwash cycle. During backwash, as water flowed up from the bottom inlet through the sand bed, the difference between the pressures measured by the two sensors was the backwash head loss.

2.4.3 Performance analysis

During the filtration cycle, performance of the filter was quantified as the negative logarithm of the fraction of remaining turbidity pC^* (often referred to as log removal), as in Eq. (2.7):

$$pC^* = -\log\left(\frac{\text{Effluent Turbidity}}{\text{Influent Turbidity}}\right) \quad (2.7)$$

The effluent turbidity was also compared to the applicable U.S. drinking water standard, which specifies less than 0.3 NTU in 95% of samples and less than 1 NTU at all times (US EPA, 2010).

Performance of the SRSF during the backwash cycle was observed to determine the extent to which the filter bed had fluidized and to monitor whether contaminants had been removed from the bed. The expansion of the bed was measured, and the expanded bed porosity ε_{Exp} was calculated for each bed expansion according to Eq. (2.8):

$$\varepsilon_{Exp} = 1 - \frac{D}{D_e}(1 - \varepsilon) \quad (2.8)$$

where: the settled-bed porosity ε was assumed to be 0.4, D is the depth of the filter (1.2 m for the six-layer system), and D_e is the expanded bed depth. In addition, data from the backwash effluent turbidimeter (shown in Fig. 2) was used to calculate the amount $M_{Removed}$ of retained contaminants that had been flushed

from the bed, as in Eq. (2.9):

$$M_{Removed} = Q_{Backwash} \sum_{t=0}^{t_{Backwash}} NTU_t \Delta t \quad (2.9)$$

where: $Q_{Backwash}$ is the backwash flow rate, NTU_t is the measured backwash turbidity at any time t , and Δt is the time interval between data points (5 s in this study). In essence, Eq. (2.9) is an integral of the turbidity vs. time function over the period of $t_{Backwash}$ for which the backwash was run. The result of this calculation has units of NTU-L, which is approximately proportional to contaminant mass because NTU is closely related to volumetric suspended solids concentration (Davis and Cornwell, 2008).

2.4.4 Field demonstration unit

An additional SRSF unit was utilized for a field demonstration. This filter was constructed using a 3" (7.62 cm) clear PVC pipe, with six 20-cm filter layers. The smaller 3" diameter column was selected for easier transportation and setup at water treatment plants in the field. Otherwise, this field demonstration unit was run under similar conditions as the laboratory SRSF: it was loaded at 1.83 mm/s (160 m/day) per layer during filtration and backwashed at 11 mm/s (950 m/day), and it used the same filter media and inlet/outlet pipes as the laboratory filter.

The filter was tested at several municipal drinking water treatment plants in Honduras that were designed and built in conjunction with the Cornell University AguaClara program. These facilities treat surface water supplies by coagulation/flocculation, sedimentation, and disinfection. The plants have capacities ranging from 6-55 L/s. They are located in small towns and cities, and each plant serves several thousand residents (Weber-Shirk, 2011). Additional information about the AguaClara program can be found at <http://aguaclara.cee.cornell.edu>.

The demonstration SRSF was connected via a siphon to the top of the upflow sedimentation tanks at each plant, as shown in Fig. 3. The filter then treated settled waters with turbidities from 1-5 NTU. The settled water was also used for backwashing. The filter was positioned so that sufficient head would be available to fluidize the sand bed; that is, a head of $HL_{Backwash}$ was available over the height of the backwash trough to provide for expansion of the sand bed as illustrated in Fig. 3. In this demonstration SRSF, the settled sand bed occupied the 1.2 m distance H_{Filter} between the lowest and highest inlets, so about 1.2 m of head was required to backwash the filter as shown in Eq. (2.6). During filtration cycles, samples were taken from the filtered effluent and measured for turbidity using hand-held turbidimeters (MicroTPW, HF Scientific) to assess the performance of the SRSF.

2.5 Results and Discussion

2.5.1 Filtration cycle performance

The laboratory SRSF treated water over a range of influent turbidities and filtration velocities comparable to typical conditions for rapid sand filtration, as shown in Table 2.3. The filtration test results presented below show that the SRSF can effectively treat settled water and can meet applicable standards for water quality. The SRSF treatment process performs at or near the level of conventional rapid sand filters, and acceptable performance is possible with the novel stacked configuration. The SRSF removed suspended solids in experiments with influent turbidity as high as 12 NTU and produced treated effluent around 0.1-0.3 NTU, showing that the SRSF process is appropriate for the typical range of rapid sand filter influent turbidities. Observations for an example experiment are shown in Fig. 2.4(a) where influent and effluent turbidities are plotted as a function of time and reveal

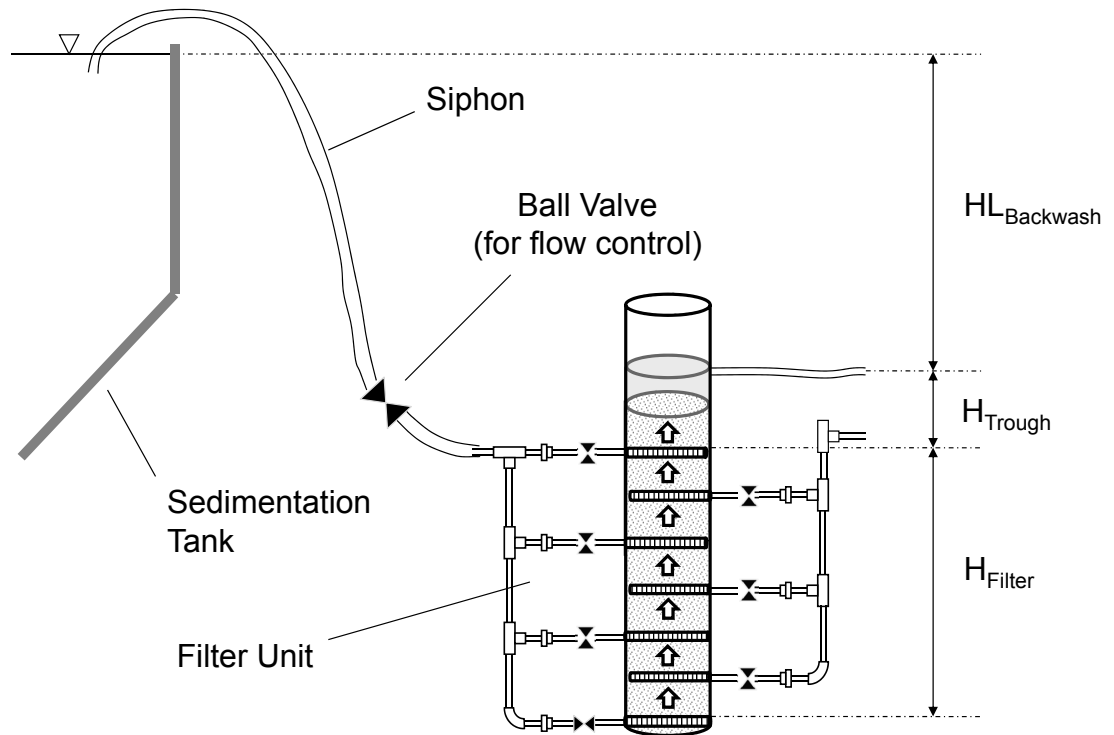


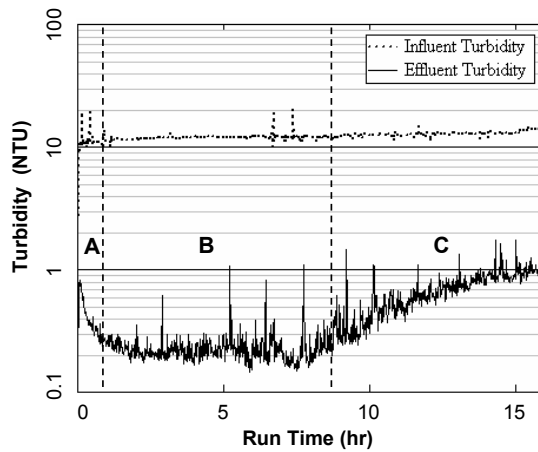
Figure 2.3: Diagram of the SRSF field demonstration unit showing its connection to the water treatment plant sedimentation tank. The flow directions and head requirement for the backwash cycle are shown here to illustrate the constraint on vertical placement of this filter. The filter bed is drawn in expanded form, but note that the height H_{Filter} is defined as the settled bed height.

Table 2.3: Bench-scale SRSF performance under various filtration-cycle conditions.

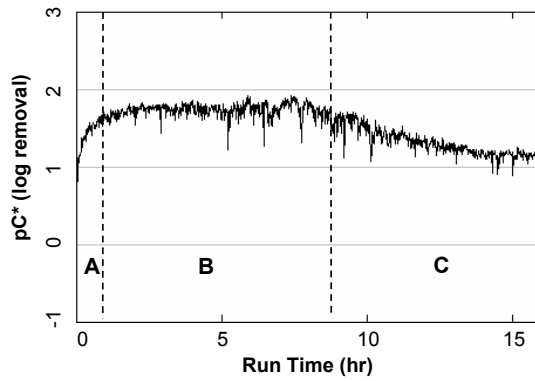
Filtration Velocity (m/day)	Previous Backwash Cycle Water	Post-ripening Averages			Samples above 0.3 NTU (%)	Length of Run (hr)
		Influent (NTU)	Effluent (NTU)	pC*		
120	Clean (tap)	5.53	0.14	1.61	0.2%	24.3
160	Clean (tap)	5.84	0.13	1.65	0.8%	25.2
160	5 NTU	5.22	0.11	1.69	0.1%	20.9
144	Clean (tap)	10.7	0.16	1.84	4.4%	10.1
144	Clean (tap)	12.0	0.24	1.70	13.5%	9.6
144	10 NTU	11.6	0.17	1.83	6.4%	9.8

a ripening period (Region A) leading to a consistent effluent turbidity around 0.2 NTU (Region B). After 10 hours of run time the performance decreased with the onset of particle breakthrough from the filter bed (Region C). In Fig. 2.4(b), the calculated pC* shows performance consistent with conventional filters. The SRSF achieved a pC* of 1.6-1.8, which corresponds to a high percent removal of turbidity (97.5-98.5%). This percent removal is within the expected range for rapid sand filters (Reynolds and Richards, 1996). Conventional filters are expected to produce better quality water than the SRSF because each layer of the SRSF is shallower than a conventional filter bed, but the turbidity removal performance of the SRSF is still satisfactory for drinking water treatment applications.

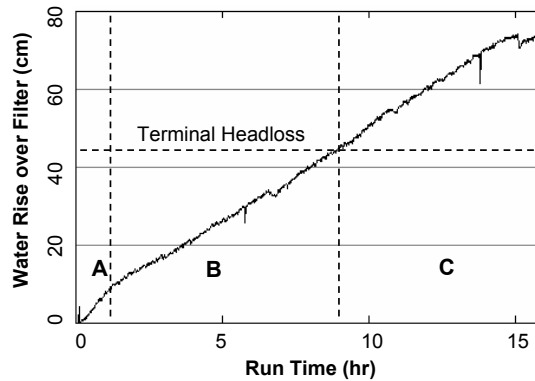
Increased head loss accompanies particle removal by a filter, as the suspended particles and coagulant retained in the sand bed create a greater resistance to flow. Fig. 2.4(c) shows a roughly linear head loss increase during the course of the filtration cycle, which is the head loss pattern that is expected for effective depth filtration (Baumann and Oulman, 1970). In design of rapid sand filters, the head loss increase is an important parameter governing the length of the filtration cycle: a terminal head loss is specified, and the filter is to be backwashed when the head loss reaches this value. The filtration cycle shown in Fig. 2.4 would produce water of appropriate quality with less than 43 cm specified as the terminal head



(a) Influent and effluent turbidity



(b) Log turbidity removal



(c) Head loss increase over the initial 15 cm clean bed head loss

Figure 2.4: Data from an example filtration cycle run at 144 m/day. The three regions demarcated on these graphs are (A) a ripening period, (B) a period of good filter performance, and (C) a decline in turbidity removal. Note that these regions are demarcated with respect to the U.S. EPA drinking water standard of 0.3 NTU.

loss, and a similar terminal head loss was observed for the other filtration trials. Note that the head loss during filtration mode through the SRSF is lower than in a conventional rapid sand filter because the filter media depth per layer is smaller in the SRSF, and total head loss is proportional to depth.

Over the course of several trials, the performance study yielded a consistent filter bed capacity (defined here as the product of turbidity removed and run time) of around 100 “NTU-hr.” The treated effluent in the example in Fig. 2.4 meets EPA drinking water standards of <0.3 NTU for a period of approximately 10 hours with 12 NTU influent, while other experiments with influent turbidity of 5 NTU allowed the SRSF a run time of more than 20 hours before needing backwash. The “NTU-hr” parameter is a property of the particular influent water used in these trials, so terminal head loss is considered a better determiner of filtration cycle time. It should be generally noted, however, that the SRSF is expected to have a shorter cycle time than a conventional filter. The SRSF has reduced bed capacity because of its shallower layers and smaller total sand volume compared to conventional technology (as shown in Table 2.2).

2.5.2 Backwashing bed expansion

A stacked filter can be effectively fluidized for backwashing just like a conventional rapid sand filter. The novel concept of performing backwash and filtration at the same total flow rate is viable from the perspective of the physical process of backwashing. There are some physical backwashing characteristics, however, that are unique to the SRSF system.

Typical backwash velocities of 10-12 mm/s (860-1000 m/day) were found to be effective in achieving bed expansion within the recommended design range of 15-30% (Davis and Cornwell, 2008). Traditional rapid sand filter design relates

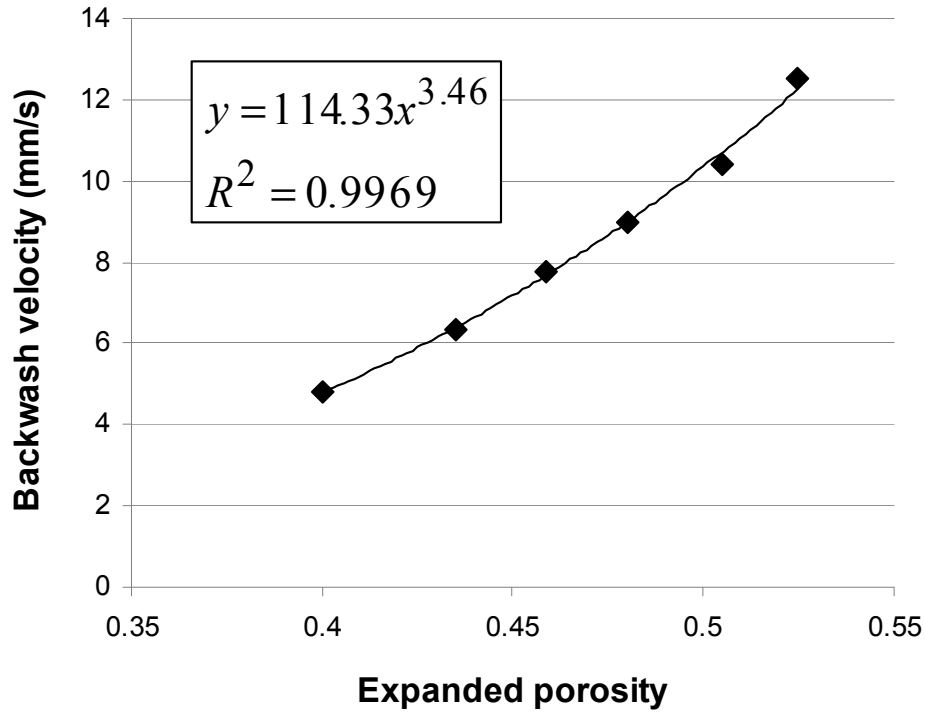


Figure 2.5: Plot of expanded porosity for increasing backwash velocities, showing experimental data points and a power-law regression equation. The initial porosity of the bed when fully settled during a filtration cycle was 0.4, and expanded porosity was calculated from measured bed expansion using Eq. 2.8.

backwash velocity to expanded-bed porosity with an empirical power-law equation of the following form (Weber, 1972):

$$V_{Backwash} = K_e (\varepsilon_{Exp})^{n_e} \quad (2.10)$$

The bed expansion of the laboratory SRSF was measured across a range of upflow velocities. A regression analysis generated the values $K_e = 114.33$ mm/s and $n_e = 3.46$ (Fig. 2.5), and the experimental data fit the model in Eq. 2.10 quite well ($R^2 = 0.997$). While the specific values of K_e and n_e are a function of the particular sand medium used in a given filter, the SRSF displays the same general relationship between backwash velocity and bed expansion as in conventional rapid sand filters.

Table 2.4: Observed bed expansion at two backwash velocities.

Inlets Closed	Layers Fluidized	Bed Expansion	
		10 mm/s	11 mm/s
1	2	9%	11%
1,2	4	16%	20%
1,2,3	6	21%	27%

Note: Inlets are numbered as in Fig. 6. Bed expansion is reported as a percent of the total 1.2 m sand bed depth.

The measured head loss for backwashing was around 1.18 m, also consistent with typical rapid sand filters and with the prediction of Eq. (2.6). The head required to fluidize the SRSF is slightly less than the 1.2 m height of the sand bed, which reflects the volume of sand displaced by the inlet and outlet pipes in the sand bed. A unique property of the SRSF system is that its fluidization can be controlled to occur two layers at a time. Table 2.4 shows the observed expansion as the six-layer laboratory SRSF was fluidized in two-layer increments. This feature stems from the configuration of inlets and outlets: each layer will fluidize when it experiences the full backwash velocity at the inlet below it, regardless of the status of the other layers of the filter. This, in turn, depends on the state of the inlet valves during backwash mode, as illustrated in Fig. 6. Similar observations were made for settling the sand bed after backwashing: (1) opening an inlet valve allows the layers below that inlet to settle, and (2) opening an outlet valve allows the layers above that outlet to settle. Opening an inlet valve reduces the flow to layers below that inlet, and therefore the velocity that these layers experience; similarly, opening an outlet allows flow out of that outlet and reduces the velocity experienced in the layers above.

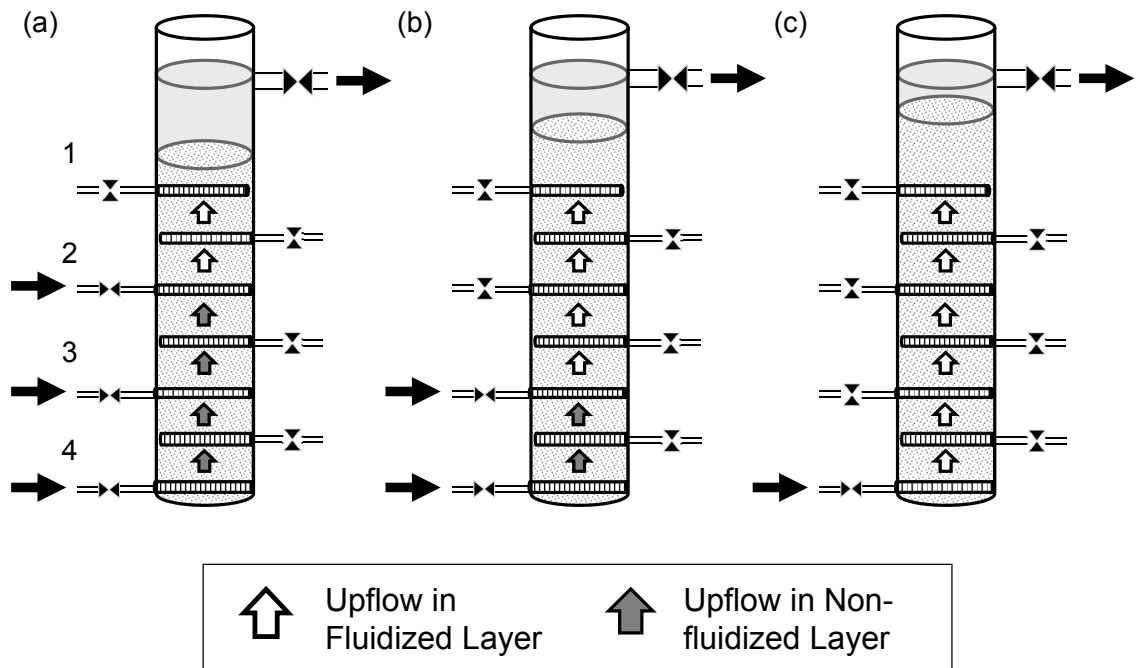


Figure 2.6: Configuration of the inlet valves of an SRSF to fluidize (a) two layers, (b) four layers, and (c) all six layers. When the inlet valves are set such that the entire backwash flow is passing upwards through a pair of layers, these layers will fluidize because they are experiencing the full backwash velocity.

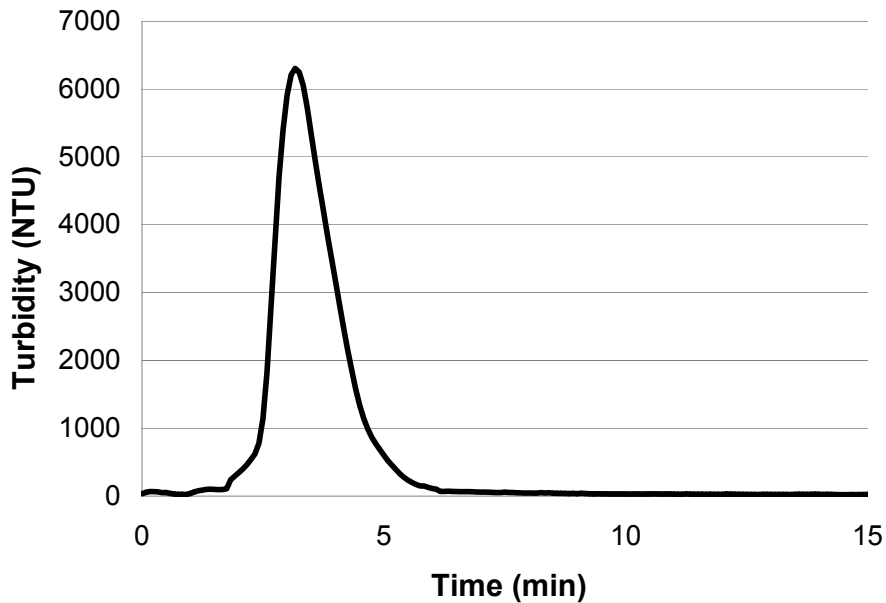


Figure 2.7: Plot of effluent turbidity over time during a 950 m/day backwash cycle. The readings from the backwash turbidimeter were scaled by the sampling system dilution factor to produce the curve shown in this graph.

2.5.3 Contaminant removal during backwash

The removal of contaminants from the filter bed was successfully demonstrated with the laboratory SRSF, and the bed fluidization was sufficient to clean the sand bed in preparation for another filtration cycle. In Fig. (2.7), the turbidity of backwash effluent is shown over the course of a backwash cycle with all six filter layers fluidized, to illustrate the removal of suspended solids that had been retained in the sand bed during filtration. The contaminants were flushed out over a relatively short period of time, producing a concentrated waste stream with a turbidity as high as 6200 NTU at its peak.

Virtually all of the contaminants loaded to the filter bed were removed during this test. During the filtration cycle preceding the filter backwash, 110 NTU influent was pumped into the filter over a period of 1.5 hours at 4.8 L/min (144 m/day), while the filter produced 1 NTU effluent. These observations correspond

to a total solids loading of 47,000 NTU-L. A total suspended solids recovery of 46,500 NTU-L (i.e., 98.9% recovery) was observed during the backwash cycle in Fig. (2.7).

In practice, the length of the backwash cycle should be minimized to reduce loss of water to backwash effluent. Fig. (2.7) shows that a 15-minute backwash cycle, as used in this test, is much longer than needed. About 94% of the solids loaded to the bed had been removed after 5 minutes of backwash, and about 97% had been recovered at 7 minutes. This suggests that for the conditions used in this research, a 7 minute backwash cycle time would be sufficient, and any additional backwashing would consume water without providing much added benefit in the form of cleaning the sand bed.

2.5.4 Use of settled water for backwash

Loss of filtered water during operation of the SRSF in the field can be reduced if sedimentation tank effluent is used to backwash the filter. When a filtration cycle ends, water would continue flowing from the sedimentation tanks into the filter at the same flow rate, but it would be redirected to the bottom inlet to fluidize and backwash the SRSF. This backwash method was evaluated to determine if it diminished the performance of the filter.

In several laboratory experiments the SRSF was backwashed with the same 5-10 NTU simulated settled water that served as influent during the filtration cycle. Results suggest that a stacked filter can be effectively backwashed with settled water without its performance being affected. As shown in Table 2.3, the pC* and effluent turbidity achieved during a filtration cycle did not change significantly after backwashing with 5-10 NTU water. The ripening time also was not noticeably affected. An interpretation of this result is that the turbidity in the

settled influent water is small compared to the large amount of turbidity in the filter bed at the onset of backwash and does not significantly affect the flushing of contaminants from the filter. In addition, most suspended particles introduced into the filter bed with the backwash water are effectively retrained by the filter media when the filtration process resumes.

If backwash is to be performed with settled water in the field, eliminating contact of backwash water with clean-water plumbing becomes an important design consideration. The placement of a trough or channel for filtered water must be such that backwash effluent will not have a path to mix with treated water for distribution. In addition, a short “filter-to-waste” period, lasting perhaps 1-2 filter residence times, is recommended to rinse the SRSF inlet and outlet pipes which were exposed to backwash water. These practical issues must be addressed as the SRSF system moves toward full-scale implementation.

2.5.5 Field demonstration results

The field demonstration was carried out to test the performance of the SRSF at operating drinking water treatment facilities, under the conditions it would face at a full-scale installation. The results from the laboratory studies indicate that both the filtration and backwash cycles can be successfully carried out in the field, and the SRSF field test was expected to produce water meeting EPA standards for turbidity. Some variation from laboratory results was anticipated, because parameters such as the total sand bed capacity vary depending on the nature of the suspended particles in the influent water.

The first test site for the SRSF demo unit was the AguaClara water treatment plant in Támara, Francisco Morazán, Honduras. Settled water from the Támara plant had turbidity in the 2-3 NTU range, which meets the Honduran standard of

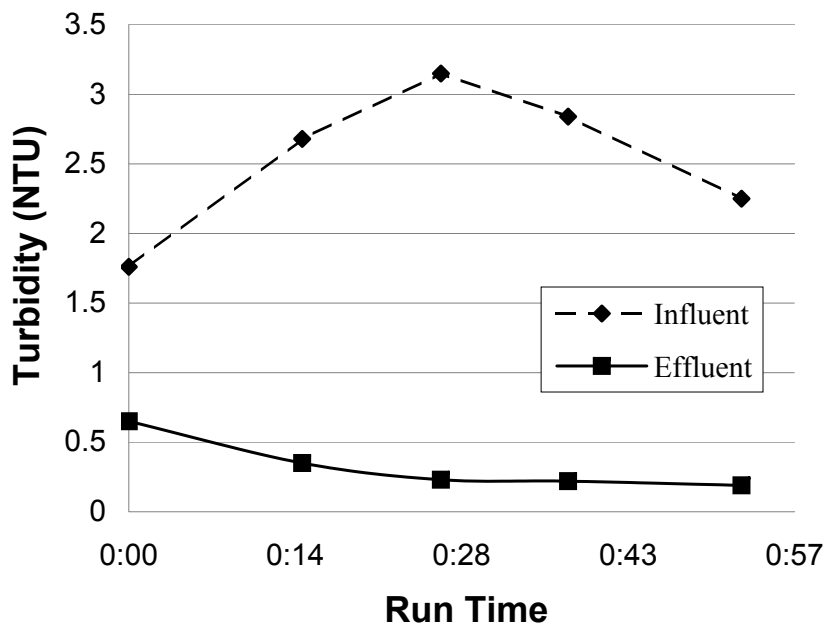


Figure 2.8: Results of the first SRSF field demonstration at the Támara water treatment plant in Francisco Morazán, Honduras, where the filter was loaded at 160 m/day with sedimentation tank effluent for around 1 hour to gauge the turbidity-removal performance of the system.

5 NTU for treated water, with about 0.5 mg/L alum residual. Filtration of this water was quite effective – in the first test (Fig. 2.8) the filter ripened in about 20-25 minutes to produce water less than 0.3 NTU, and achieved effluent quality as low as 0.19 NTU. In the second test (results not shown), the filter ran overnight producing water around 0.5 NTU. The run concluded after about 18 hours, as the head loss in the filter increased 28 cm and the effluent turbidity approached 1 NTU.

At the AguaClara water treatment plant test site in Agalteca, Francisco Morazán, Honduras, settled water turbidity was in the 0.5-1 NTU range. SRSF filtration was initially not effective with the cleaner influent water in Agalteca, and a 1 mg/L dose of alum was then added to the filter influent for part of the test. In samples without alum addition, there was no discernable or consistent difference

between the influent and filtered water; with alum added, the filter performed consistently better and achieved as low as 0.31 NTU effluent. These results indicate that addition of alum to the influent can improve filter performance when needed. Similar results for coagulant addition to rapid sand filters have been demonstrated in laboratory and full-scale pilot tests reported by Lin et al. (2011).

2.6 Conclusions

Stacked rapid sand filtration is presented in this paper as a robust and sustainable technology that can address the limitations of conventional rapid sand filtration for municipal drinking water treatment facilities around the world. Backwashing conventional rapid sand filters requires expensive systems such as electric pumps, elevated storage tanks, or large banks of parallel filters. A stacked rapid sand filter, meanwhile, is self-backwashing at the same flow rate used for filtration, and it does not require pumps or other electrical equipment.

Effective backwashing bed expansion, efficient removal of contaminants from the sand bed during backwash, and adequate filtration-cycle performance of the SRSF system have been demonstrated in the laboratory and in field tests. Because the SRSF concept has been shown to be viable, it could be used at full scale to realize significant benefits relative to conventional filters: reduced complexity of implementation and operation; savings in capital and operating costs, and possible reductions in water lost to backwashing.

Further research should consider the design and operational details required for implementation of a full-scale stacked rapid sand filter. In addition, laboratory investigation of issues such as alum-filter interaction, flow distribution among filter layers, and backwashing hydraulics can help to optimize the technology.

2.7 References

- Ahrens, B. T. and Mihelcic, J. R. (2006). “Making wastewater construction projects sustainable in urban, rural, and peri-urban areas.” *Journal of Engineering for Sustainable Development: Energy, Environment, Health*, 1(1), 13–32.
- American Society of Civil Engineers (ASCE) (2009). “2009 Report Card for America’s Infrastructure.” *Infrastructure Report Cards*, <<http://www.infrastructurereportcard.org/report-cards>> (May 24, 2011).
- American Water Works Association (AWWA) (1971). *Water Quality and Treatment*. McGraw-Hill, New York, 3rd edition.
- Arora, H., Giovanni, G. D., and LeChevallier, M. (2001). “Spent filter backwash water contaminants and treatment strategies.” *Journal of the American Water Works Association*, 93(5), 100–112.
- Baumann, E. R. and Oulman, C. S. (1970). *Sand and diatomite filtration practices*. Water Quality Improvement by Physical and Chemical Processes, University of Texas Press, Austin, TX.
- Cornwell, D. A. and MacPhee, M. J. (2001). “Effects of spent filter backwash recycle on Cryptosporidium removal.” *Journal of the American Water Works Association*, 93(4), 153–162.
- Davis, M. L. and Cornwell, D. A. (2008). *Introduction to Environmental Engineering*. McGraw-Hill, New York, 4th edition.
- Foote, J., Baker, C., and Bordlemay, C. (2010). “Drinking Water Quality Report.” *Annual Water Quality Report 2010*, Bolton Point Municipal Water System, City of Ithaca Water System, and Cornell University Water System, <<http://www.boltonpoint.org/waterquality.html>>.

- Gitis, V. (2008). "Rapid sand filtration of *Cryptosporidium parvum*: effects of media depth and coagulation." *Water Science and Technology - Water Supply*, 8(2), 129–134.
- Hokanson, D. R., Zhang, Q., Cowden, J. R., Troschinetz, A. M., Mihelcic, J. R., and Johnson, D. M. (2007). "Challenges to implementing drinking water technologies in developing world countries." *Environmental Engineer: Applied Research and Practice*, 43, 31–38.
- Lin, P. H., Lion, L. W., and Weber-Shirk, M. L. (2011). "Comparison of the ability of three coagulants to enhance filter performance." *Journal of Environmental Engineering*, 137(5), 371–376.
- Mihelcic, J. R., Fry, L. M., Myre, E. A., Phillips, L. D., and Barkdoll, B. D. (2009). *Field Guide to Environmental Engineering for Development Workers*. ASCE Press, Reston, VA.
- Mintz, E., Bartram, J., Lochery, P., and Wegelin, M. (2001). "Not just a drop in the bucket: expanding access to point-of-use water treatment systems." *American Journal of Public Health*, 91(10), 1565–70.
- Nasser, A., Huberman, Z., Dean, L., Bonner, F., and Adin, A. (2002). "Coagulation as a pretreatment of SFBW for membrane filtration." *Water Science and Technology - Water Supply*, 2(5-6), 301–306.
- Reynolds, T. D. and Richards, P. A. (1996). *Unit Operations and Processes in Environmental Engineering*. PWS Publishing Co., Boston.
- Stillwell, A. S., King, C. W., Webber, M. E., Duncan, I. J., and Hardberger, A. (2010). "The energy-water nexus in Texas." *Ecology and Society*, 16(1).

- U.S. Environmental Protection Agency (US EPA) (2010). “Drinking Water Contaminants.” *Office of Groundwater and Drinking Water*, <<http://water.epa.gov/drink/contaminants/index.cfm>> (October 17, 2010).
- Weber, W. J. (1972). *Physiochemical Processes for Water Quality Control*. Wiley-Interscience, New York.
- Weber-Shirk, M. L. (2011). “Concept Paper: Municipal Water Projects and Open Source Engineering.” *Cornell University AquaClara*, <<https://confluence.cornell.edu/display/AGUACLARA/Publications>> (April 9, 2011).
- Whittington, D. and Hanemann, W. M. (2006). *The economic costs and benefits of investments in municipal water and sanitation infrastructure: a global perspective*. CUDARE working paper series 1027, University of California, Berkeley.
- Yang, C. B., Cheng, Y. L., Liu, J. C., and Lee, D. J. (2006). “Treatment and reuse of backwash water in Taipei water treatment plant, Taiwan.” *Water Science and Technology - Water Supply*, 6(6), 89–98.
- Yao, K. M., Habibian, M. T., and O’Melia, C. R. (1971). “Water and waste water filtration: concepts and applications.” *Environmental Science and Technology*, 5(11), 1105–1112.

CHAPTER 3

A NOVEL FLUIDIC CONTROL SYSTEM FOR AGUACLARA STACKED RAPID SAND FILTERS

3.1 Abstract¹

Infrastructure for water treatment faces numerous challenges around the world, including the high failure rate of digital, electronic, pneumatic, and mechanical control systems due to their large number of components and their dependency on proprietary parts for repair. The development of more efficient, reliable, easily-repaired water treatment controls that rely on simple fluidics rather than on sophisticated systems has the potential to significantly improve the reliability of drinking water treatment plants, particularly for cities and towns in developing countries. The AguaClara stacked rapid sand filter (SRSF) has been proposed as a more robust and sustainable alternative to conventional rapid sand filters because each filter can backwash at the same flow rate used for filtration without requiring pumps or storage tanks. The viability of stacked rapid sand filtration has been demonstrated through previous laboratory studies and at a municipal water treatment plant. This paper presents a novel control system for the SRSF based on fluidics. The fluidic control system, which permits changing between the filtration and backwash modes of operation with a single valve, was developed in the laboratory and applied in the first full-scale SRSF. The water level in the filter is regulated by a siphon pipe, which conveys flow during backwash and which contains an air trap to block flow during filtration. The state of the siphon pipe and the ensuing state of the filter is controlled by one small-diameter air valve.

¹The contents of this thesis chapter have been submitted to the *Journal of Environmental Engineering*, with co-authors M.L. Weber-Shirk, J.C. Will, A.N. Cordero, W.J. Maher, and L.W. Lion

3.2 Introduction

In many cities and towns, drinking water infrastructure is inadequate, underperforming, or technically deficient (Lee and Schwab, 2005). Failure of water treatment systems is part of the reason why an estimated 1.8 billion people lack access to safe drinking water (Onda et al., 2012). Moreover, the high capital and operating costs of water treatment systems have been identified as major barriers to their more widespread implementation in developing countries (Hokanson et al., 2007). In industrialized countries, water treatment systems are more widely available, but there is nevertheless a significant need of capital for maintenance and for new water infrastructure in the coming decades (ASCE, 2009).

Water treatment plants that rely on digital, electronic, pneumatic, and mechanized control systems have multiple failure modes that result in a short mean time between repair events. The failures of mechanized plants are due to component failures, reliance on proprietary parts that are unavailable in the local supply chains, high energy costs, and designs that fail to provide adequate feedback to the operator for successful water treatment. For example, 20 modular mechanized water treatment plants were installed in Honduran cities in a program that ended in 2008. By the beginning of 2012, 50% of the plants had been abandoned due to control system failures and significant energy costs (Smith, D.W., 2012, Agua Para el Pueblo-Honduras, personal communication).

The choice of technology is a crucial factor to achieve sustainability for water projects (Breslin, 2003), and the use of technology that is inappropriate for its context has been implicated as the reason for many failures of infrastructure systems (Moe and Rheingans, 2006). Water treatment plants can be designed for sustainable operation and a long useful life by simplifying the control system, eliminating dependence on electricity, minimizing the number of moving parts, designing the

unit processes to provide operator feedback, using locally available materials, and simplifying operation and maintenance procedures. Although water treatment plant mechanization and automation might normally be expected to reduce labor requirements and thus operating costs, the need for highly skilled professionals with different expertise to maintain the control systems of automated plants may actually increase labor costs. In addition, the parts required for automated systems are not readily available in many parts of the world.

The need for resilient water treatment plant designs that are high-performing with low capital and operating costs led to the search for an improved filtration design by the AguaClara program at Cornell University in 2010. Initial evaluation of existing technologies revealed none meeting these requirements. Slow sand filters require too much level land (a scarce resource in mountainous terrain) to treat large flow rates, and rapid sand filters require either enclosed filter vessels, pumps, large storage tanks, or sets of six filters working together to achieve the high velocities required for backwash. The capital costs of the rapid sand filter options are high, often out of reach for small to mid-size communities, and the closed-vessel pressure filter option does not give plant operators visual feedback on the condition of the filtration system. For this reason, pressure filters are not considered appropriate for normal surface water treatment, and design guidelines limit their use to iron and manganese removal (WSCGL, 2007).

The AguaClara stacked rapid sand filter (SRSF) was invented to address the need for a robust, lower cost, high-performing, and sustainable alternative to conventional rapid sand filters (Adelman et al., 2012). The SRSF uses the same flow rate for the filtration and backwash cycles, and it therefore does not require the pumps or elevated storage tanks needed to backwash conventional filters. The SRSF works by placing inlets and outlets made of well-screen pipe within the filter

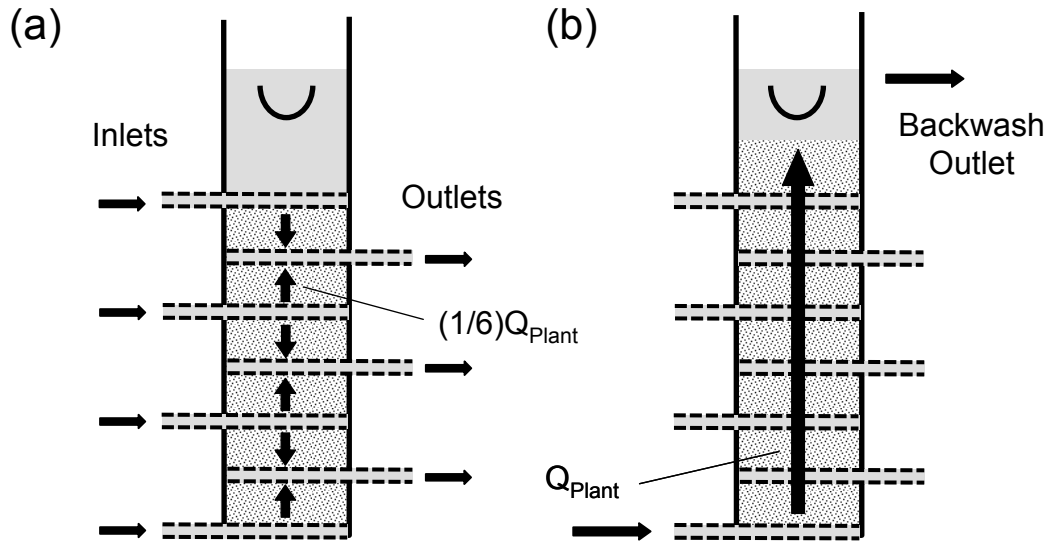


Figure 3.1: Diagram of flow in the sand bed of an SRSF during (a) filtration and (b) backwash. Note that the total incoming flow rate Q_{Plant} is the same during both cycles of operation.

sand bed, creating multiple layers that filter in parallel but that are backwashed in series. Using the same flow rate for both cycles, the SRSF achieves a backwash velocity equal to the number of layers times the filtration velocity. The typical design ranges of filtration and backwash velocities for rapid sand filtration differ by approximately a factor of six, making six filter layers a reasonable choice for design. Flow through the bed of a six-layer SRSF during the filtration and backwash cycles is shown in Figure 3.1.

The viability of the SRSF was first demonstrated through laboratory studies and a small-scale field demonstration by Adelman et al. (2012), and the first generation full-scale 12 L/s SRSF was built in 2011 at the municipal water plant serving the town of Támara, Francisco Morazán, Honduras (Will et al., 2012). The initial report of the SRSF by Adelman et al. discussed the requirement for flow to be provided to the layers of the sand bed as shown in Figure 3.1, but no control system was proposed to achieve this. This paper presents a novel system of fluidics

to control the SRSF, supported by theoretical analysis, experimental demonstrations, and full-scale implementation. This system consists of inlet and outlet boxes with riser pipes and a siphon with an air valve to control the mode of operation. The fluidic control system eliminates the need for digital, electronic, pneumatic, or other mechanized controls and allows the operator to select the mode of operation of the filter with a single small-diameter air valve.

3.3 Materials and Methods

3.3.1 Pilot-scale apparatus

A pilot-scale apparatus (Figure 3.2) was developed for laboratory studies of the proposed fluidic control system, starting from the apparatus used by Adelman et al. (2012) for the original proof-of-concept studies. The SRSF in this system was built in a 4" (10.16 cm) diameter clear PVC column with six 20 cm layers. The inlet and outlet pipes were 1/2" (1.27 cm) PVC with 0.2 mm well-screen slots spaced at 1/8" (0.318 cm) provided by Big Foot Mfg. in Cadillac, MI. The sand bed consisted of typical rapid sand filter sand, with an effective size of 0.45 mm and a uniformity coefficient of 1.4 (Ricci Bros. Sand Co., Port Norris, NJ). Water was applied to this filter at a total flow rate of 5.3 L/min, giving a backwash velocity of 11 mm/s when the flow passed through all layers in series and a filtration velocity of 1.83 mm/s when the flow was divided among the six layers. These values are consistent with typical design values for filtration and backwash velocities in single-media rapid sand filters (Reynolds and Richards, 1996).

The experimental apparatus also included fluidics controls to set the mode of operation of the SRSF by controlling air entry to and exit from a siphon system. Important components of this fluidics control system are shown in Figure 3.2,

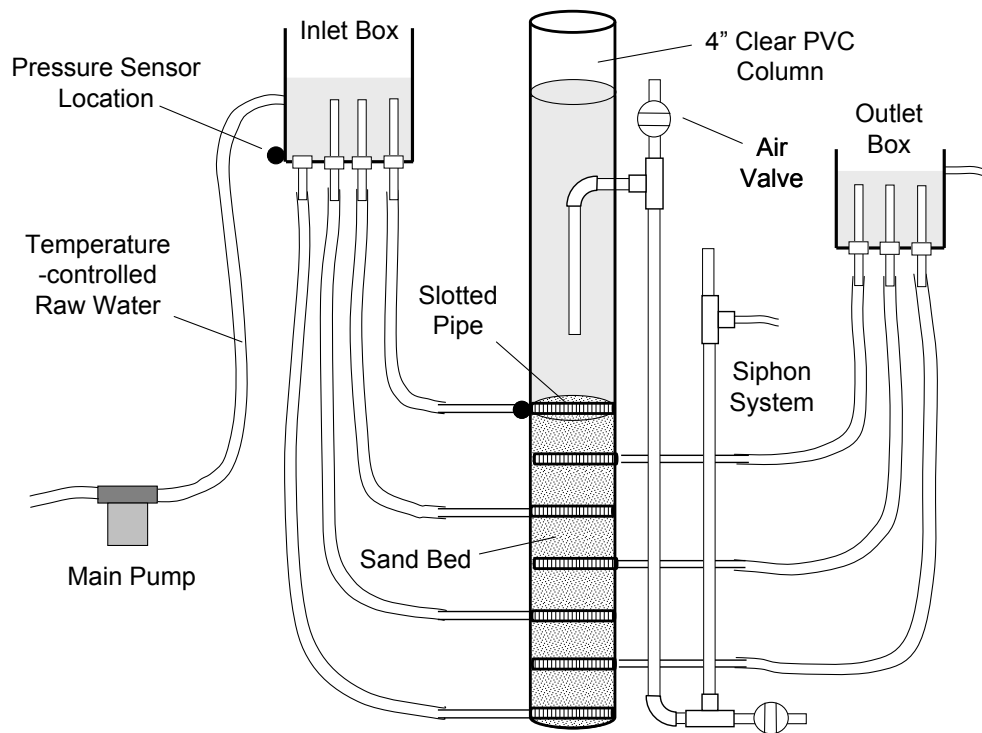


Figure 3.2: Pilot-scale experimental apparatus including an SRSF column, inlet and outlet boxes, a backwash siphon, an air valve, and pressure sensors. Note that the water levels shown here are for the filtration cycle.

including an inlet box where water enters the SRSF from upstream processes, an outlet box for filtered water, a backwash siphon, and an air valve. These components regulate the water levels and flow paths during each cycle of operation.

3.3.2 Control of parameters and data acquisition

Raw water for the laboratory apparatus came from a temperature-controlled reservoir which blended hot and cold tap water to achieve a room temperature mix. This prevented excess dissolved gases in the cold tap water from influencing the hydraulics of the system. The tap water came from the Cornell University water system, and had an average pH of 7.7 with roughly 150 mg/L as $CaCO_3$ of hardness and 120 mg/L as $CaCO_3$ of alkalinity (Foote et al., 2012). The pump shown in Figure 3.2 was used along with a flow control valve to supply water to the inlet box at a constant rate of 5.3 L/min. In the municipal scale filter discussed below, the inlet box is gravity-fed by placement just below the sedimentation tank outlet, and no pumping of water is required.

Important water levels in the system were tracked using differential pressure sensors (PX26 series, Omega Engineering Inc., Bridgeport, NJ). These sensors were installed at the locations indicated in Figure 3.2, with their positive side connected via fittings to the inlet box or filter column and their negative side exposed to the atmosphere to correct for variations in atmospheric pressure. The sensors were calibrated to measure pressure in units of centimeters of water, so that the water level could be tracked in the inlet box and the filter column during experiments. Data from these pressure sensors was logged to a computer via the laboratory process control and data acquisition system described by Weber-Shirk (2009).

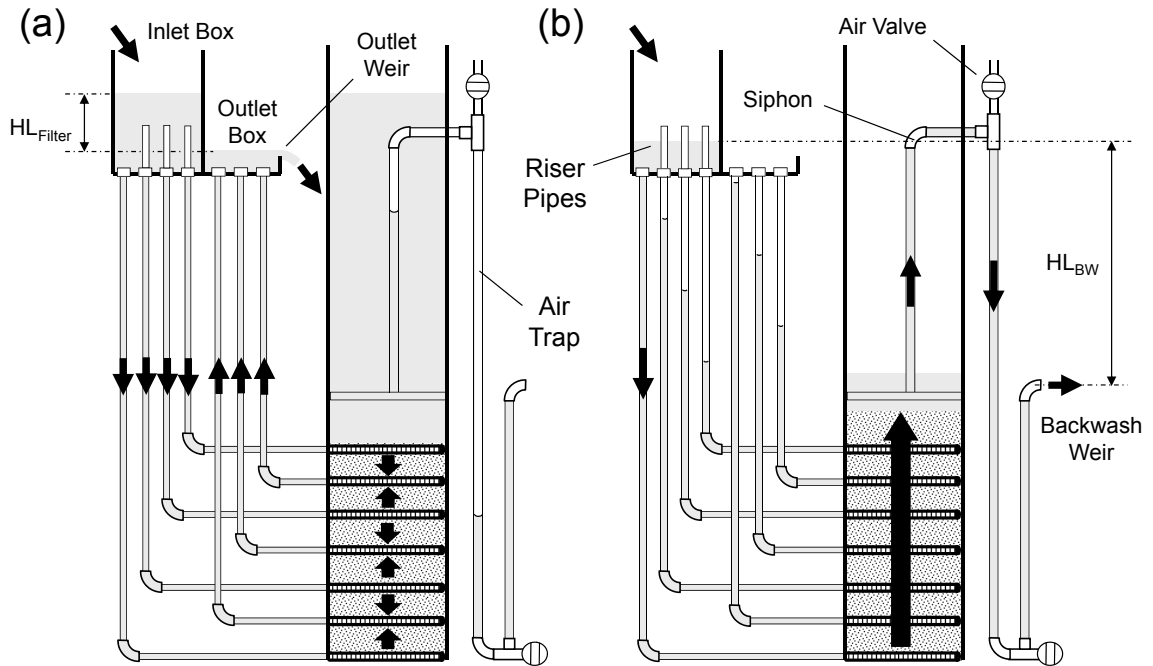


Figure 3.3: Fluidics control system for the SRSF, showing water levels during (a) filtration and (b) backwash. Important head losses during each cycle are also identified.

3.4 Results and Discussion

3.4.1 Overall control system

The SRSF fluidic control system uses the backwash siphon to set the water level in the filter and thereby control the mode of operation (Figure 3.3). Only one valve is required to operate this filter - the air valve used to fill or empty the siphon pipe by establishing or releasing an air trap.

When the siphon pipe is blocked by air, the SRSF is in filtration mode. Water is forced to exit over the weir in the outlet box, and the water level in the inlet box and in the filter are high enough to overcome the filtration head loss HL_{Filter} . This head loss is attributable to flow through the inlet and outlet plumbing, slotted pipes, and sand bed along any one of the six parallel paths through the filter. The clean

bed head loss during the filtration cycle can be estimated with familiar models such as the Carmen-Kozeny equation or the Rose equation (see, for example, Reynolds and Richards, 1996).

When there is water flow in the siphon, the SRSF is in backwash mode. The water level in the filter is just high enough for flow to pass through the siphon and exit the system over the backwash weir. The water level in the inlet box drops until it provides the total required backwash head loss HL_{BW} . The head h_L required to fluidize a sand bed of depth H_{Sand} is given by Equation (3.1):

$$h_L = H_{Sand} (1 - \varepsilon) \left(\frac{\rho_{Sand}}{\rho_{Water}} - 1 \right) \quad (3.1)$$

where ε is the porosity of the sand, ρ_{Sand} is the sand density, ρ_{Water} and is the density of water. Based on both typical properties of filtration sand and on experimental observation, h_L is approximately equal to the depth of the sand bed in both conventional and stacked rapid sand filters (Adelman et al., 2012). The total backwash head loss includes losses in the inlet plumbing or siphon pipe. The riser pipes on the entrance to the top three inlets prevent these inlets from receiving flow during backwash, causing all flow to be directed to the bottom inlet in order to fluidize the sand filter media and backwash the filter.

3.4.2 Experimental evidence of mode transitions

The effectiveness of the fluidic control system to set the mode of operation of the filter was confirmed using the laboratory apparatus. Figure 3.4 shows the temporal variation of the water level in the inlet box and the filter column as the control system was used to set both cycles. In the experiment shown, the SRSF started in filtration mode, was changed to backwash, and then was returned to filtration. Water levels in the figure are measured relative to the top of the settled sand bed.

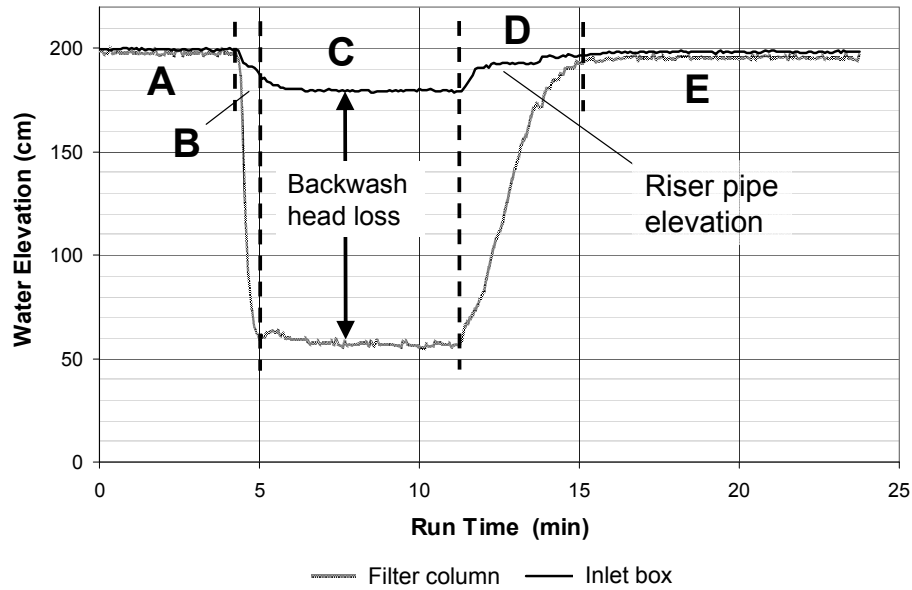


Figure 3.4: Water level traces from the pilot-scale apparatus, showing the water level change in the inlet box during the change from filtration to backwash and the return to filtration mode of operation.

The data presented in Figure 3.4 is divided into five “zones” illustrating the important steps in the transition between filtration and backwash cycles using the fluidics control system:

- *Zone A.* The system is in filtration mode, with the water level high enough in both the inlet box and the filter column for flow to exit over the outlet weir. The inlet box level is a few centimeters above the water level in the filter column, which represents the head loss in the inlet plumbing. The top of the siphon pipe is completely submerged by the water in the filter column, but is maintaining an air trap to prevent water from escaping to the backwash weir.
- *Zone B.* The air valve is opened and then closed over an interval of approximately 5 s. This time interval is also used in the full-scale SRSF. Opening the air valve allows the trapped air to escape, so that the siphon can fill

and water can begin flowing out over the backwash weir. Once there is flow in the siphon, the water level quickly drops from its former level above the siphon pipe in both the filter and the inlet box. This transition takes about 1 minute in the laboratory filter and about 3 minutes in the field.

- *Zone C.* The system is in backwash mode. The water level in the filter column is a few centimeters above the elevation of the backwash weir, representing the head loss in the siphon pipe. The water level in the inlet box is high enough to provide the 1.2 m backwash head loss (equal to the depth of the sand bed), but below the top of the highest three riser pipes. This directs all flow from the inlet box to the bottom inlet of the filter.
- *Zone D.* The air valve is opened and then closed, again for about 5 s in the lab and the field. This allows air to be pulled into the siphon, cutting off flow in the siphon pipe and re-forming the air trap. Because the water can no longer exit via the backwash siphon, it must rise in both the inlet box and the filter column so it can once again exit over the outlet weir. The elevation of the riser pipes in the inlet box is evidenced by the short horizontal section on the inlet box curve, between about 12 and 14 minutes of run time.
- *Zone E.* The system has returned to filtration mode. Once again, the height of water in the filter column reflects the elevation of the outlet weir plus the clean-bed filtration cycle head loss.

This data in Figure 3.4 provide good evidence that the fluidic control system works as proposed. The effectiveness of this control system was also confirmed by the success of the SRSF in the field. The first full-scale SRSF in Támara can successfully transition between filtration and backwash just as was observed in the pilot-scale system (Will et al., 2012).

3.4.3 Fluidic control of the mode of operation

Controls based on fluidics are used to select which inlets and outlets are active during filtration and backwash modes. Flow to the top three inlets must cease during backwash so that all of the water is forced into the bottom of the filter. The top three inlets are turned off by lowering the water in the inlet box to be below the level of the three inlets, as shown in Figure 3.3(b). It is also important that outlet pipes not be hydraulically connected during backwash, to prevent backwash water from preferentially traveling through the pipes instead of through the fluidized sand bed. The outlet pipes are disconnected from each other by lowering the water level in the outlet box to be below the top of the outlet pipes.

The successful transition in flow was based on an analysis to determine the relevant head losses in the system. The placement of the inlet box and the length of the riser pipes depend on both the filtration and backwash cycle head losses. In addition, the energy losses between the entrance to the bottom inlet manifold and the siphon exit can be used to estimate where the water levels will be in the unused inlet and outlet pipes during backwash. The water levels in these pipes are illustrated in Figure 3.3(b), and the outlet box must be placed as shown in the figure to prevent short-circuiting during backwash.

Changes in water levels in the transition from filtration to backwash mode are set by the siphon and controlled by the air valve. To initiate backwash, the air valve opens the siphon pipe, closes three inlet pipes, closes three outlet pipes, and increases the flow rate through the bottom filter inlet. To initiate filtration, the air valve closes the siphon pipe, opens three inlet pipes, and opens three outlet pipes. The use of fluidics thus eliminates seven large-diameter valves - one on each inlet pipe and each outlet pipe - that would otherwise be required to control filter operation.

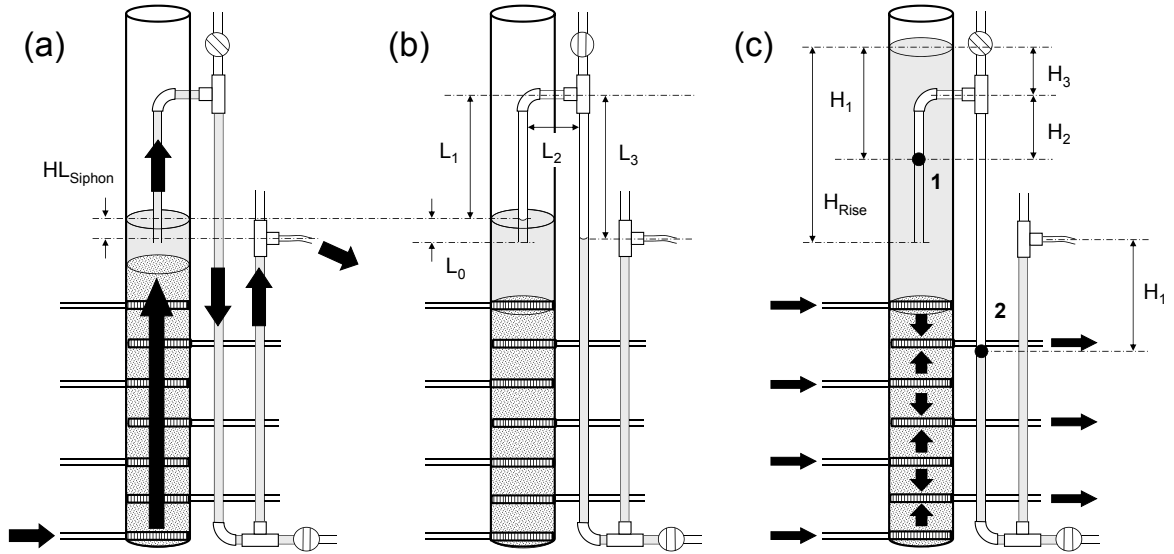


Figure 3.5: Diagram of flow and water levels in the siphon pipe and key dimensions, including (a) during the backwash cycle, (b) just after the siphon is broken to end backwash, and (c) after water has risen to the clean-bed filtration height.

3.4.4 Backwash siphon air trap hydrostatics

The siphon pipe and its air trap are the central elements of the SRSF fluidic system, and the design of this siphon is critical to the operation of the control system. The hydrostatics of the SRSF siphon were characterized in the laboratory apparatus. Figure 3.5 shows the siphon during backwash mode, the initial air volume that is taken into the pipe just after the air valve is opened to cut off backwash flow, and the hydrostatic equilibrium observed during the filtration cycle.

At the end of the backwash cycle, the siphon is broken by opening the air valve. Because the siphon is under negative gauge pressure when it is conveying backwash water, as in Figure 3.5(a), air will enter the pipe when the air valve is opened. The initial volume of air that is pulled into the siphon pipe at the end of the backwash cycle occupies the lengths L_1 , L_2 , and L_3 in the siphon pipe, as shown in Figure 3.5(b). As the SRSF transitions to filtration mode and the water

level rises (Zone D in Figure 3.4), this air volume is pushed along the siphon into the position shown in Figure 3.5(c).

The siphon pipe geometry must be designed so that the air trap can be maintained as the water level rises in the filter box. The lower U-shaped portion of the siphon pipe remains filled with water that acts as a “water seal,” and the back pressure on this side of the pipe must be sufficient to resist the pressure exerted on the air trap by the water in the filter column. The density of air is sufficiently small compared to the density of water that the pressure can be assumed to be constant in the air trap, so the hydrostatic pressures at points 1 and 2 in Figure 3.5(c) must balance:

$$P_1 = P_2 = \rho_{Water}gH_1 + P_{Atm} \quad (3.2)$$

where P_1 and P_2 are the absolute pressures at points 1 and 2, P_{Atm} is atmospheric pressure, ρ_{Water} is the density of water, g is the gravitational acceleration, and H_1 is the length defined in Figure 3.5(c). Because the pressures balance as shown in Equation (3.2), the difference in height from the water in the filter column to point 1 and the vertical displacement of the water seal from the backwash weir to point 2 will have an identical value H_1 . The increase in hydrostatic pressure will cause the air in the trap to compress slightly from its initial volume:

$$P_{Atm}V_{Initial} = P_1V_{Compressed} \quad (3.3)$$

where $V_{Initial}$ is the initial air volume and $V_{Compressed}$ is the volume of the air trap in its compressed state. From the geometry of the system, the initial volume in the air trap is approximately:

$$V_{Initial} = A_{Siphon}(L_1 + L_2 + L_3) \quad (3.4)$$

where A_{Siphon} is the cross-sectional area of the siphon pipe and L_1 , L_2 , and L_3 are the pipe lengths defined in Figure 3.5(b). Note that this initial air volume is conservatively taken to exclude the length L_0 that remains submerged as a result of the water level in the column during backwash. Once the water has risen in the filter as in Figure 3.5(c), the air volume is:

$$V_{Compressed} = A_{Siphon} (L_2 + L_3 + H_1 + H_2) \quad (3.5)$$

where H_2 is the distance between the water level in the upstream side of the siphon pipe and the horizontal section of the siphon pipe.

The system of Equations (3.2) through (3.5) can be used to analyze the equilibrium condition in the siphon pipe at any point during filtration. Substituting Equations (3.2), (3.4), and (3.5) into Equation (3.3) and dividing through by A_{Siphon} gives:

$$P_{Atm} (L_1 + L_2 + L_3) = (\rho_{Water} g H_1 + P_{Atm}) (L_2 + L_3 + H_1 + H_2) \quad (3.6)$$

A useful result of Equation (3.6) is that it is possible to solve for the position of water levels in the siphon pipe, given the height of water in the filter, H_{Rise} . In order to do this, H_2 is defined geometrically as:

$$H_2 = L_0 + L_1 - (H_{Rise} - H_1) \quad (3.7)$$

where H_{Rise} is the height of water in the filter from the inlet of the siphon pipe. If the water in the column has risen by a given amount H_{Rise} , Equation (3.7) can be substituted into Equation (3.6) to eliminate all unknowns except for H_1 :

$$P_{Atm} (L_1 + L_2 + L_3) = (\rho_{Water} g H_1 + P_{Atm}) (L_0 + L_1 + L_2 + L_3 + 2H_1 - H_{Rise}) \quad (3.8)$$

It is therefore possible to find the position of the water levels on both sides of the siphon pipe by solving for H_1 in Equation (3.8).

An important failure mode can also be identified from Equation (3.6) - that is, the height of water H_3 that will cause water to begin spilling over into the horizontal section of the siphon pipe. This is the maximum water height that the air trap can resist before failing, and it can therefore be used as a design constraint to select an appropriate vertical geometry of the siphon system. This failure mode takes place when H_2 goes to zero, so the maximum value of H_3 is found by subjecting Equation (3.6) to this condition and noting that when $H_2 = 0$, H_1 must be equal to H_{3Max} :

$$P_{Atm} (L_1 + L_2 + L_3) = (\rho_{Water} g H_{3Max} + P_{Atm}) (L_2 + L_3 + H_{3Max}) \quad (3.9)$$

Given the geometry of an SRSF siphon, Equation (3.9) can be solved for H_{3Max} , the maximum height of water that the air trap can support during a filtration cycle.

The siphon was evaluated experimentally in laboratory tests to validate this model. Following a backwash cycle, the water was allowed to rise in the column, and the locations of water levels in the siphon system were measured. Dimensions of the experimental siphon and the lengths measured during this experiment are shown in Figure 3.6.

For four different heights H_{Rise} of water in the column, the lengths a , b , and c were measured, and Equation (3.8) was solved to predict these lengths given the physical dimensions of the siphon in Figure 3.6(a). For these calculations, we used the dimensions of the apparatus $L_0 = 6 \text{ cm}$, $L_1 = 1.30 \text{ m}$, $L_2 = 16 \text{ cm}$, and $L_3 = 1.32 \text{ m}$, and an atmospheric pressure of $P_{Atm} = 1 \text{ atm}$. The results of this experiment are shown in Table 3.1. The measured values of a and c were the same at each point as predicted by Equation (3.2), and the model underestimated the measured values of a , b , and c by 3-6%. The error in the predicted values comes from our estimate of the initial air volume in the siphon pipe - in reality, this initial

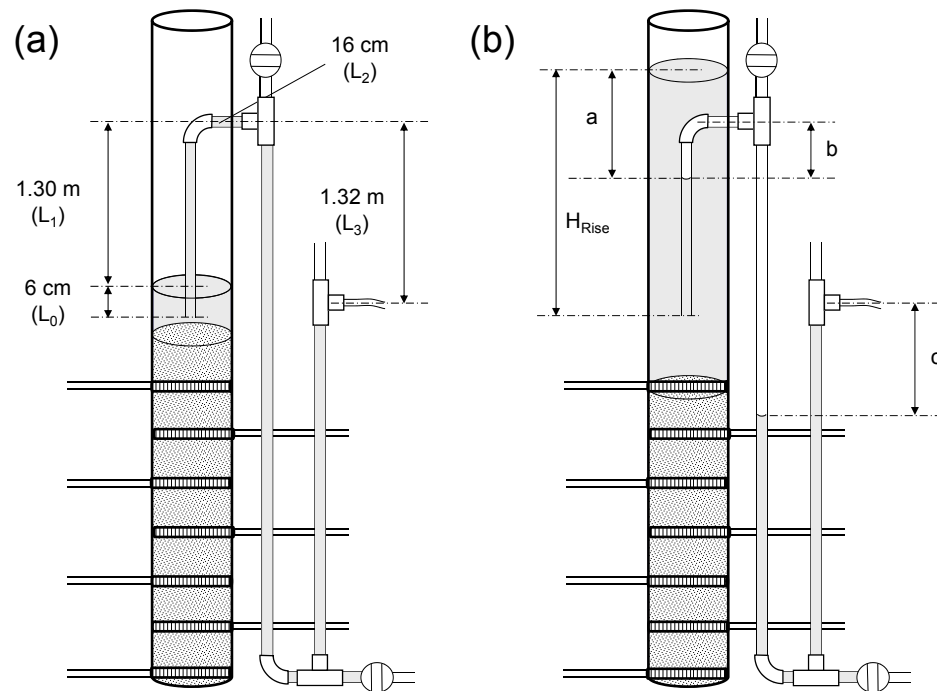


Figure 3.6: Diagram of (a) dimensions and (b) observed water levels for the laboratory-scale siphon system. The water in the filter column was allowed to rise a height H_{Rise} over the top of the sand, and the lengths a , b , and c were measured.

Table 3.1: Predicted and measured values of a and b in the experimental siphon, given H_{Rise}

H_{Rise} (cm)	a (cm)		b (cm)		c (cm)	
	Predicted	Measured	Predicted	Measured	Predicted	Measured
107.8	45.1	47.6	73.2	75.8	45.1	47.6
125.0	52.7	55.2	63.7	66.2	52.7	55.2
142.5	60.6	63.2	54.1	56.7	60.6	63.2
168.0	71.9	74.5	40.0	42.5	71.9	74.5

air volume is larger than the volume shown in Figure 3.5(b), because the water passing through the U-shaped tube on the outside of the filter has momentum when the siphon is broken and it is expected to fall below the levels shown in the figure. However, our estimate of the initial air volume represents a minimum value, and it would therefore be appropriate to use the model for a conservative design.

3.4.5 Backwash siphon air valve sizing

The state of operation of the entire system is controlled by the air valve on the backwash siphon. This valve must accomplish two key functions. The first is to allow the air in the siphon trap to escape when the filter is to be backwashed, as at the beginning of Zone B in Figure 3.4. The second is to break the siphon and pull in a new volume of air when backwash is finished and a new filtration cycle is to be started, as in Zone D.

The first function is readily accomplished. When the air valve is opened, the positive gauge pressure on the air trap forces the air to be quickly expelled into the atmosphere. To accomplish the second function, the air valve must allow a sufficient volume of air to enter so that the air trap can be re-formed in a reasonable amount of time. The desired flow rate of air to break the siphon and re-establish the air trap therefore sets the minimum required diameter of the air valve. The

target air flow rate Q_{Target} of air is based on a desired time t_{Design} to fill the siphon:

$$Q_{Target} = \frac{V_0}{t_{Design}} \quad (3.10)$$

where V_0 is the initial air volume defined in Equation (3.4).

In addition to the target flow rate, sizing this valve requires that the relevant driving head and head losses be identified. The initial driving head h_0 in this situation is a result of the negative gauge pressure in the upper portion of the siphon during backwash:

$$h_0 = \Delta z_{Valve} + \frac{V_{Siphon}^2}{2g} + h_{LSiphon} \quad (3.11)$$

where Δz_{Valve} is the elevation of the air valve tee over the backwash water level in the filter column, V_{Siphon} is the flow velocity of water in the siphon, and $h_{LSiphon}$ is the head loss between the siphon entrance and the air valve tee. This equation is dimensionally consistent, as long as all lengths and head losses are expressed in consistent units (e.g. cm of water). When the air valve is initially opened there is a net pressure of h_0 forcing air into the system, but once the siphon pipe is filled with air, the pressure in the pipe approaches 1 atm and the driving head drops to zero. Therefore, the air valve should be designed for an initial flow rate of twice the target flow, because this will produce an average flow of Q_{Target} over a period of t_{Design} , given that the driving head will decline from h_0 to zero. Because minor losses dominate over the short length of the air valve pipe, the minimum size of the air valve D_{Valve} can be calculated with a minor loss equation:

$$D_{Valve} = \sqrt{\frac{Q_{Design}}{\pi}} \left(\frac{8K}{gh_{L0Air}} \right)^{1/4} \quad (3.12)$$

where $Q_{Design} = 2Q_{Target}$; the coefficient K incorporates all minor losses along the path of air entering the system, including the air pipe entrance, the air valve itself, the air pipe exit, and any other adaptors or fittings; and h_{0Air} is the initial driving

head h_0 from Equation (3.11) converted into units of air:

$$h_{0Air} = \left(\frac{\rho_{Water}}{\rho_{Air}} \right) h_0 \quad (3.13)$$

where ρ_{Air} is the density of air.

In the field, the goal to minimize air valve size was motivated by the desire to reduce construction costs. Using a wood board and hole saws to replicate the orifice size of standard ball valves, a series of tests were performed on the full-scale filter starting with a 3" PVC ball valve and covering the siphon opening with successively smaller orifices. The tested hole sizes included 2", 1 1/2", 1", 3/4", and 1/2" nominal pipe sizes. Both initiation and breaking of the siphon were tested to ensure that neither transition would fail due to insufficient air leaving or entering the siphon. Successful termination of backwash was defined as having the water from the vertical section of the siphon pipe return to the filter box, indicating that the water in the siphon had been displaced by air.

Observations in the field showed that the air valve could be as small as a 1/2" brass ball valve (actual diameter 19/32" or 1.508 cm). No further testing was done with smaller valves, not only because the 1/2 in valve met the goal of cost reduction and no smaller valve sizes were readily available, but also because the time to initiate and terminate backwash would be unacceptably long for smaller orifice sizes. The full-scale siphon has an air trap volume of approximately 44 L and a fill time of 5.6 s, yielding an average air flow rate of 7.8 L/s. The initial driving head of $h_0 = 1.25 \text{ m}$ for air flow into the full-scale siphon gives a K value of 2.65 in Equation (3.12). This is consistent with the nature of the minor losses in the system: the entrance to the air pipe could be thought of as a projecting entrance with $K = 1$, the exit from the air pipe into a much lower velocity zone would have an additional $K = 1$, and there is some additional minor loss attributable to the open ball valve.

3.5 Conclusions

A novel system of fluidic controls has been developed for the SRSF to set its mode of operation, and this system has been successfully deployed at a municipal water treatment plant. The fluidic control mechanism is based on a siphon pipe controlled by an air trap and by water levels changes that are designed to automatically control three inlets and three outlets. The use of a single small-diameter air valve to fill and empty the siphon with air simplifies operation and completely eliminates all of the failure modes associated with digital, electronic, and pneumatic controls that are common in mechanized water treatment plants. In addition, the cost of the air control valve is negligible in comparison with conventional digital, electronic, and pneumatic control systems. This novel system was tested in pilot-scale experiments, which demonstrated the transition between the filtration and back-wash cycles. Physical models were proposed for the hydrostatics of the siphon and for air flow in the control valve, and these models were validated by observations with the laboratory and full-scale systems.

3.6 References

- Adelman, M. J., Weber-Shirk, M. L., Cordero, A. N., Coffey, S. L., Maher, W. J., Guelig, D., Will, J. C., Stodter, S. C., Hurst, M. W., and Lion, L. W. (2012). “Stacked filters: a novel approach to rapid sand filtration.” *Journal of Environmental Engineering*, in press.
- American Society of Civil Engineers (ASCE) (2009). “2009 Report Card for America’s Infrastructure.” *Infrastructure Report Cards*, <<http://www.infrastructurereportcard.org/report-cards>> (May 24, 2011).
- Breslin, E. D. (2003). “The demand-responsive approach in Mozambique: why choice of technology matters.” *UNICEF-Waterfront*, 16, 9–12.
- Foote, J., Baker, C., and Bordlemay, C. (2012). “Drinking water quality report.” *Annual Water Quality Report 2012*, Bolton Point Municipal Water System, City of Ithaca Water System, and Cornell University Water System, <<http://www.ci.ithaca.ny.us/departments/dpw/water/report.cfm>>.
- Hokanson, D. R., Zhang, Q., Cowden, J. R., Troschinetz, A. M., Mihelcic, J. R., and Johnson, D. M. (2007). “Challenges to implementing drinking water technologies in developing world countries.” *Environmental Engineer: Applied Research and Practice*, 43, 31–38.
- Lee, E. J. and Schwab, K. J. (2005). “Deficiencies in drinking water distribution systems in developing countries.” *Journal of Water and Health*, 3(2), 109–27.
- Moe, C. L. and Rheingans, R. D. (2006). “Global challenges in water, sanitation and health.” *Journal of Water and Health*, 4, 41–58.
- Onda, K., LoBuglio, J., and Bartram, J. (2012). “Global access to safe water:

- accounting for water quality and the resulting impact on MDG progress.” *International Journal of Environmental Research and Public Health*, 9(3), 880–894.
- Reynolds, T. D. and Richards, P. A. (1996). *Unit Operations and Processes in Environmental Engineering*. PWS Publishing Co., Boston.
- Water Supply Committee of the Great Lakes (WSCGL) (2007). “Recommended Standards for Water Works.” *Ten State Standards*, <<http://10statesstandards.com/waterstandards.html>> (June 18, 2012).
- Weber-Shirk, M. L. (2009). “An automated method for testing process parameters.” *Cornell University AguaClara*, <<https://confluence.cornell.edu/display/AGUACLARA/Process+Controller+Background>> (June 18, 2012).
- Will, J. C., Adelman, M. J., Weber-Shirk, M. L., and Lion, L. W. (2012). “Implementation of the AguaClara stacked rapid-sand filtration process at the municipal water treatment plant in Tamara, Francisco Morazan, Honduras.” *XXVII Congreso Centroamericano de Ingenieria Sanitaria y Ambiental*, San Salvador, El Salvador (March 2012).

CHAPTER 4

OVERALL CONCLUSIONS AND IMPLICATIONS

4.1 Conclusions of the Two Studies

Taken together, these two studies describe the SRSF and provide evidence for the effectiveness of the two key innovations upon which it depends. The novel geometry of the sand bed creates six layers using four inlets and three outlets, and it is possible to use the same flow rate to achieve good quality water during filtration and clean the sand bed during backwashing. The fluidic control system provides the required flow patterns during both filtration and backwash, and the single air valve on the backwash siphon pipe sets the mode of operation by controlling flow to all of the inlets and outlets.

The results of these studies were applied to bring the SRSF to scale. The sand bed geometry found to be effective in Chapter 2 was applied to a field-scale filter, where the vertical arrangement of six layers at 20 cm each was the same and the plan-view area was scaled to the flow rate to be treated. The required area of the full-scale SRSF was sized based on the desired backwash velocity, and the selection of a typical rapid sand filter backwash velocity gave an acceptable loading rate for filtration as well. The fluidic control system described in Chapter 3 is also scalable. The physical models developed for the backwash siphon air valve and air trap hydrostatics were used to produce a full scale control system design, and were effectively applied to the first full-scale SRSF in Támara.

4.2 Future Work for Laboratory Research

Continued laboratory research on the SRSF will be required to gain a better fundamental understanding of the technology and to further refine its design and

operation. Important questions for ongoing laboratory research include:

- *Layer flow distribution.* The calculation of the filtration loading rate relies on the implicit assumption that flow is equally divided among the six layers, and it stands to reason that this will be the case as long as head loss along each path through the filter is dominated by identical layers of sand. However, there would be value in further empirical and theoretical investigation of this issue to develop a clear design guideline for the inlet and outlet plumbing.
- *The self-healing nature of flow distribution problems.* Even if the flow in an SRSF is not distributed evenly among the six layers, it is possible that this is a 'self-healing' problem. A layer with higher flow would entrain and accumulate suspended solids at a higher rate than a layer with lower flow, so the head loss coefficient for the path through the higher-flow layer would likely increase at a greater rate. Ultimately, this effect would be expected to push the system back towards even flow distribution, but further experimental observation is needed to determine whether this is the case. Preliminary data from pressure sensors in each layer of the pilot-scale SRSF suggests that this self-healing effect does indeed occur in a stacked filter.
- *Upflow and downflow performance.* Further testing can show whether or not there are relevant differences in turbidity removal performance between upflow and downflow layers in the SRSF. It is also worth investigating how the nature of the upflow layers affects the terminal head loss for the SRSF filtration cycles. When increased head loss during a filtration cycle leads to a hydraulic gradient near of near 1 cm head loss per 1 cm of layer depth in the upflow layers, it is possible that these layers may start to lift or shift and release entrained particles. Preliminary bench-scale data implies that the turbidity removal performance of upflow and downflow layers is virtually

identical, but more data is needed on the question of terminal head loss.

- *Layer configuration.* The geometry proposed in Chapter 2 of six layers at 20 cm each appears to provide for both reasonable loading rate and layer depth. Given that an eight-layer SRSF would have to be unreasonably deep, the only other reasonable configuration would involve four layers. It is possible that four 20 cm layers is a viable configuration, but if a backwash velocity of 11 mm/s is selected to provide adequate bed expansion for cleaning, the loading rate during the filtration cycle would be higher than the recommended range for rapid sand filtration. Preliminary data from a four-layer SRSF suggests that the high filtration velocity does in fact adversely affect particle removal, and leads to inadequate filter performance.
- *Sand media selection.* It would be useful to specify guidelines for appropriate sand media to be used in the SRSF. The effective diameter of the media affects many design and operating parameters including the required backwash velocity, the run time, and the head losses; the uniformity is also important, because a highly varied media may stratify significantly and lead to mal-distribution of flow in different layers of the SRSF.

Beyond its self-backwashing nature, the SRSF may have some additional fundamental advantages. Firstly, there is virtually no surface removal observed during the filtration cycle. This stands to reason because all flow is injected into the filter bed at high velocity from the slotted pipes, thus eliminating areas of the filter where surface removal could occur. In conventional filtration theory, the entrainment of suspended particles of any type by depth-removal mechanisms leads to a linear increase in head loss over the course of a constant-rate filter cycle. This is consistent with the SRSF performance data presented in Chapter 2.

In addition, the four influent injection points would lead to four zones in the SRSF where entrained solids are concentrated at the end of the filtration cycle, as opposed to one such zone in conventional filters. The SRSF may therefore produce a more concentrated waste stream during backwash, which would lead to reduced required volume to flush out each unit mass of contaminant. Both the elimination of surface removal and the production of more concentrated backwash water must be further investigated before they can be claimed as advantages of the SRSF.

4.3 Future Work for Field Implementation

Additional research with the full-scale filter in Támara will also be important to address practical issues related to fabrication of parts, maintenance, and operation. Building and running the filter at scale involves a host of challenges that cannot be addressed simply through laboratory research, and the experience in Támara has certainly produced - and will continue to produce - important lessons to improve the implementation of future filters.

The filter has performed well in the field so far, producing water significantly below the U.S. EPA standard for turbidity. It therefore represents a major water quality improvement for the AguaClara treatment plants. However, some important lessons have already been learned through the first full-scale implementation. The original design of the filter inlet box specified a weir too close to the inlet riser pipes, which led to significant air entrainment and reduced both particle removal performance and filtration cycle run time. This weir was removed to correct the problem, and the layout of the inlet box for future filters must consider the possibility that air may enter the sand bed if there is a zone of highly turbulent flow too close to the inlet pipes.

One other important lesson learned concerns the fabrication of inlets and outlets for the filter. The original design used a trunk pipe along one wall of the filter box with slotted pipes attached perpendicularly, along with a series of elbows and tees to support the slotted pipes at the opposite wall. Unfortunately, the connections to the trunk pipe were not sufficiently sand-tight, and the length of filtration cycles was reduced by sand entering the manifolds. Some pipes also broke out of their tee connections because they had been slotted all the way to the end. In future filters, the tees and elbows will be replaced by another smaller trunk line, which will likely prove simpler to construct. Slotted pipes with short un-slotted zone at each end, along with better connections between the slotted pipes and trunk lines, will also be required.

Several other challenges remain as the SRSF moves towards more widespread implementation. Mud balls - large agglomerations of media and entrained particles - may grow large enough to escape removal during backwash and accumulate in the bottom of the filter. In many rapid sand filters, compressed air scour is used to eliminate mud balls. In the SRSF, the elimination of surface removal may prevent mud balls from forming in the first place, thus eliminating any need for air scour; however, further operational data will be needed to validate this hypothesis.

Perhaps more significantly, the outlet pipes in an SRSF are exposed to backwash water by virtue of their placement in the sand bed. This creates the risk that contaminants from the backwash water may make their way into the treated water effluent. In a conventional filter, the water at the end of a backwash cycle must pass through the sand bed again to reach the underdrain and outlet. In a stacked filter, most of the water in the box at the end of backwash is never treated - instead, it remains in the top of the filter box to be drained via the siphon pipe at the start of the next backwash - but the outlet plumbing certainly comes in

contact with backwash water. Therefore, a short filter-to-waste period is currently employed in Támara to rinse the filter plumbing and flush away any remaining contaminants, and the operator begins sending water to the distribution system only when it appears clear enough to do so. In-line continuous logging of the filter effluent turbidity in the field would be an important data collection step to ensure that the operator is using a reasonable time for filter-to-waste - sufficiently long to reduce the effluent turbidity to below acceptable standards, but not excessively long so as to waste potable water.

Finally, the presence of the filter in an AguaClara plant changes the nature of the entire process, so it is possible that plant operating parameters such as the required dosing of coagulant and disinfectant will change. With the SRSF, it should be possible for the AguaClara plants to meet EPA standards virtually all of the time, but doing so will require optimization of the treatment process at the plant scale.